Contents

Study Syllabus for Classification of Radiographs of Pneumoconioses

Introduction

Preface

A major role of the National Institute for Occupational Safety and Health (NIOSH), under the Federal Mine Safety and Health Act, is to conduct research and service programs to detect and prevent respiratory impairment and disability in coal workers. One way this responsibility has been carried out is through the administration of a health surveillance program for coal miners, including periodic chest radiographs. In 1972, NIOSH, in cooperation with the Johns Hopkins University School of Medicine, developed a proficiency examination to help identify physicians who could provide accurate and precise interpretations of chest radiographs according to the International Labour Office (ILO) Classification system. This examination was revised in 1976, 1980, and 2002 to conform to changes in the ILO Classification system and, in 2018 to align with digital radiograph technology.

We encourage physicians planning to take the latest proficiency examination to utilize this self-study syllabus as a valuable resource. Physicians are not required to complete the syllabus before sitting for the proficiency examination. However, its use, or some other means of study, is highly recommended for physicians who do not regularly use the ILO Classification system and who plan to interpret digitally acquired chest radiographs of individuals exposed to dust in an occupational setting.

Coal Workers' Health Surveillance Program
Surveillance Branch - Respiratory Health Division
National Institute for Occupational Safety and Health
cwhsp@cdc.gov
(304) 285-5724

NIOSH wishes to express deep appreciation to the following contributors:

Professional staff of the American College of Radiology (ACR) and the physician members of the ACR Taskforce on Pneumoconiosis, who generously contributed their time and expertise to develop this self-study syllabus:

ACR Staff/Consultants:
Ronald E. Freedman, Executive Vice President
Elizabeth G. Yarboro, Senior Director
Jorge Rodriguez-Guasch, Instructional Systems Developer
Matthew Wenger, Consultant, ITPG, Inc.
Robert Lissitz, Consultant

ACR Taskforce on Pneumoconiosis:
Daniel A. Henry, MD, FACR (Chair)
Kathleen A. DePonte, MD
John R. Forehand, MD
Jeffrey P. Kanne, MD
James Lockey, MD
David A. Lynch, MB, ChB
Cristopher A. Meyer, MD, FACR
Cecile S. Rose, MD, MPH
Danielle M. Seaman, MD
Ralph T. Shipley, MD
Joseph F. Tomashefski Jr, MD

Drs. Michael Attfield, Robert Cohen, Robert Tallaksen, John Parker, and Edward Petsonk for assistance in selecting radiographs from the NIOSH Chest Image Repository (CIR).

Drs. David Weissman and Douglas Johns for providing institutional support for the project.

Dr. Cara Halldin for providing project leadership.

Travis Markle, MS for providing technical support for the project.

The International Classification of Radiographs of Pneumoconioses: A Comprehensive Self-study Syllabus

The self-study syllabus intends to familiarize you with the International Classification of Radiographs of Pneumoconioses and to explain the methods used to classify radiographs of dust-exposed workers. Most importantly, it provides examples and practice images that will enable you to describe the presence, shape, size, and profusion of opacities and other findings used in the ILO classification.

To accomplish these objectives, we have divided the syllabus and illustrative radiographs into five subsets.

Subset 1 discusses the NIOSH Radiograph Classification Form, line by line and section by section. It explains the form's use and illustrates the descriptive terms employed.

Subset 2 focuses on the competent use of the classification form for the ranges of rounded and irregular small opacities at the various profusion levels.

Subset 3 allows you to classify several radiographs using the ILO system.

Subset 4 provides a narrative analysis of small rounded and small irregular opacities at the low profusion levels. These are the most challenging visual discriminations.

Subset 5 includes 34 additional radiographs and blank classification forms. It also includes validated classifications (or answer keys) by expert B Readers to assess your practical application of the ILO classification guidelines and principles presented in the syllabus.

The answer keys for classifying radiographs from Subsets 2 through 4 are in a separate document:

https://www.cdc.gov/niosh/chestradiography/php/about/index.html

Important Note: The ILO Classification system is semi-quantitative. An element of subjectivity and minor differences among readers is expected. However, if your classification differs markedly from the validated classification provided, we urge you to restudy the portions of the syllabus that deal with the area of disagreement.

Upon successful completion of this self-instructional resource, you should be able to classify radiographs of pneumoconioses in digital format competently and confidently, according to the ILO Classification system. You should also be prepared to take the B Reader proficiency examination offered by NIOSH.

The NIOSH B Reader certification and recertification examinations are regularly offered in Morgantown, West Virginia. You can find the necessary procedures and specific requirements for scheduling a NIOSH examination on the NIOSH website at B Reader Exam Overview | Radiographic Screening and B Readers | CDC.

Additional information can be obtained by telephone at (304) 285-5724.

The University of Illinois Chicago and the American College of Radiology also offer opportunities to take the examination. Information may be found at B Reading Course and Exams | Mining Education and Research Center | University of Illinois Chicago (uic.edu) and ACR Education Center in Reston – NIOSH B Reader Training and Examination | American College of Radiology.

*You may encounter minor differences between classification forms due to periodic revisions. However, the most significant components of the forms, and most importantly, the principles of classification, remain unchanged.

Getting Started

Instructions

Before getting started, please review the following information, which is designed to help you navigate the material as efficiently and effectively as possible.

Teaching Components

The self-study syllabus provides an overview of the Clinical and Pathologic Basis of selected Occupational Lung Diseases and sets of radiographs with explanations and answer keys. **The radiographs and answer keys are available as separate downloads.**
https://ftp.cdc.gov/pub/niosh-syllabus/

I. ILO International Classification of Radiographs of Pneumoconioses

The ILO Classification provides a means for systematically describing and recording radiographic abnormalities in the chest after the inhaling of dust. It is used to describe radiographic abnormalities that occur in any type of pneumoconiosis and is designed for classifying only the appearances seen on postero-anterior chest radiographs.

The ILO Classification aims to codify radiographic abnormalities of the pneumoconioses in a simple, reproducible manner. The ILO Classification is used internationally for:

- Epidemiological research.
- Screening and surveillance of workers in dusty occupations.
- Clinical purposes.

The ILO Classification consists of guidelines for using the ILO International Classification of Radiographs of Pneumoconiosis along with a set of standard radiographs. The guidelines are a technical publication designed to standardize classification methods and to facilitate international comparison of pneumoconiosis statistics and research reports.

II. Practice Radiographs

Accurate classification of findings mandates careful review of digitally acquired DICOM images and their comparisons with the ILO Standard Reference Images. It is easier to study on a workstation with multiple monitors or a wide screen. You will likely have several windows or browser tabs open to toggle between the syllabus, sample radiographs, standards, and answer keys.

First, select a medical image viewer to see the radiographs. NIOSH provides BViewer, which is a free radiograph viewer for Microsoft Windows. BViewer works best with Intel and Nvidia graphics adapters.

Instructions to install the NIOSH BViewer and ILO Standards

You may also use other medical image viewers and open on two monitors. You can use one monitor to view the syllabus, and the other monitor to view the standards.

Below is a partial list of viewers you can also use.

- MicroDicom (Windows).
- Radiant Viewer (Windows).
- FViewer (free web-based viewer).
- Imaios (free web-based viewer).
- Horos Project (iOS).

Web-based viewers may not have enough memory to load all syllabus images at one time. NIOSH suggests only loading about 20 images at a time. You will also need the following downloads if you select another viewer:

- 2022 ILO Standards.
- NIOSH B Reader Syllabus Radiographs (DICOM).
- NIOSH Chest Radiograph Classification Form.
  A fillable PDF that you may save on your local device or print.
- Answer keys for Radiographs 20 to 83.
  Radiographs 1 through 19 do not have answer keys. They are described in the syllabus.

III. Quiz

Subset 1 of the syllabus describes proper use of the classification form. A short quiz follows the syllabus. The quiz is designed to reinforce the important, preceding discussion. Expert feedback is provided to reinforce your learning.

Clinical Overview

Clinical Approach to the Diagnosis and Treatment of Occupational Lung Diseases

Introduction: Integrating Imaging and Clinical Evaluation

Chest imaging is a critical component in the clinical evaluation and epidemiologic study of occupational lung diseases. Contemporary chest imaging technology includes digital chest imaging, which can be used for classification according to the International Labour Office (ILO) system, and high-resolution chest computed tomography (HRCT). While the cost and radiation dose associated with HRCT are falling, this technology has not been adopted worldwide for medical surveillance of apparently healthy dust-exposed workers. At present, no internationally accepted classification system for HRCT compares to the ILO Classification System for plain chest radiographic images, although such a system has been proposed and evaluated in research reports [Kusaka et al. 2005].

This syllabus provides a general overview of the clinical approach to diagnosing and managing major occupational lung diseases. It focuses on the integration of imaging findings with other components of clinical evaluation, particularly the exposure history. This approach optimizes prompt and accurate diagnosis, more effective treatment, appropriate control or elimination of exposures, and other prevention efforts [Cox and Lynch 2015]. ILO classifications are primarily used for dust-exposed workers, but they have also been used to classify the pattern and extent of interstitial changes in other occupational lung diseases. This includes the granulomatous diseases associated with hypersensitivity pneumonitis and chronic beryllium disease. We have included a discussion of occupational asthma, chronic bronchitis, and emphysema in Appendix A. However, medical surveillance and diagnosis of workers at risk for these diseases rarely require chest imaging with ILO classification.

Major Occupational Lung Diseases

Pneumoconioses

Silicosis

Silicosis refers to a spectrum of lung diseases caused by inhalation of respirable crystalline silica (RCS). Workers from a broad range of industries are exposed to RCS; these include coal and hard rock mining, hydraulic fracturing, foundries, tunneling, stone and countertop cutting, sandblasting, construction and masonry, glass manufacturing, concrete and ceramics production, and agriculture.

Several clinical presentations of the disease have been described. Acute silicosis, also known as silicoproteinosis, results from exposure to high concentrations of respirable silica, with symptoms occurring within weeks to a few years after exposure onset. The diagnosis of acute silicosis is based on a history of acute, high-dose silica exposure. Imaging findings may include diffuse ground glass opacity with interlobular septal thickening (the "crazy-paving" pattern), a milky lipoproteinaceous bronchoalveolar lavage effluent, and exclusion of other potential explanations (e.g., infection, pulmonary edema, alveolar hemorrhage).

Excessive silica exposure is associated with an increased risk for lung cancer. It is also linked to autoimmune disorders (including rheumatoid arthritis, systemic sclerosis, and increased serum autoantibodies); chronic kidney disease; chronic airflow obstruction (including emphysema and chronic bronchitis); and lung infections from mycobacteria and some fungal species.

No specific treatment for acute or chronic silicosis has proven safe and effective. Lung transplantation may be an option for patients with progressive respiratory failure. Medical management targets mitigating ongoing exposure, bronchodilators if airflow limitation is present, treatment of infection, pulmonary rehabilitation, supplemental oxygen if hypoxia is present, appropriate vaccinations, and smoking cessation.

Silicosis, like all occupational pneumoconioses, is a preventable disease. Primary prevention through controlling exposures must be the highest priority. Personal respiratory protection may temporarily mitigate exposure but is an ineffective long-term solution. Medical surveillance of at-risk workers using chest radiographs and spirometry is a critical component of secondary prevention and can detect early disease. This facilitates reduction or removal from exposure of the affected worker and provides important feedback on the effectiveness of primary prevention programs.

Coal Mine Dust Lung Disease

Inhalation of coal mine dust can lead to various respiratory conditions included under the broad category of coal mine dust lung disease (CMDLD) [Petsonk et al. 2013]. Coal mine dust is a complex and variable mixture that may contain coal, silica and silicates, calcium carbonates used for rock dusting, diesel exhaust, and depending on specific conditions, other particulates and volatile chemicals. Mining methods and the coal miner's job duties, including proximity to the coal face, determine the concentration and type of exposure. Both underground and surface miners are at risk for the disease.

The spectrum of CMDLD includes coal workers' pneumoconiosis (CWP), silicosis, mixed-dust pneumoconiosis, dust-related diffuse fibrosis, and emphysema and chronic bronchitis. CWP typically requires at least 10 years of exposure to manifest chest radiographic findings, classified as small opacity (sometimes called simple) or complicated. Small opacity CWP classically manifests as small, rounded opacities, often more profuse in the upper zones (Fig. 1). The **q**-type of small, rounded opacities is associated with macules and micronodules on pathology, while **r**-type opacities are associated with macronodules [Vallyathan et al. 1996]. Although upper lung-predominant rounded opacities are more common, lower lung-predominant irregular opacities may also be seen [Blackley et al. 2015; Laney and Petsonk 2012; Young et al. 1992]. Though many patients with early small opacity CWP have normal lung function, decrements in forced expiratory volume in 1 second (FEV1), forced vital capacity (FVC), and FEV1/FVC ratio are greater with increasing profusion of small opacities [Blackley et al. 2015]. CWP can also progress to Progressive Massive Fibrosis (PMF), which has radiographic and computed tomography (CT) appearances similar to PMF caused by exposure to RCS (Fig. 2), with opacities of at least 1 cm in long axis diameter.

Large opacities typically start in the lung periphery, have a round or lentiform shape paralleling the pleura, and may enlarge over time. As a large opacity evolves, it may migrate toward the hilum, with a concomitant decrease in background small nodule profusion, and may cavitate or calcify. The large opacities of CWP may be unilateral or they may involve the lower lungs. PMF caused by coal mine dust exposure is associated with substantial impairment in lung function, often with mixed restrictive and obstructive changes and decreased diffusion capacity.

Small irregular opacities may also be an isolated radiographic finding, most commonly in the lower lungs [Cockcroft et al. 1983; Collins et al. 1988; Laney and Petsonk 2012]. While these irregular opacities can be related to smoking, some are due to lung fibrosis and can be progressive. There are reports of a pattern of diffuse interstitial fibrosis characterized by lower lung predominant fibrosis (**Fig. 3**), with histology similar to usual interstitial pneumonia, including peripheral subpleural honeycombing, traction bronchiectasis, and ground glass opacity [Brichet et al. 1997; Honma and Chiyotani 1993; Katabami et al. 2000]. This pattern is known as dust-related diffuse fibrosis. Recognizing this pattern is important as it may be associated with lung cancer [Katabami et al. 2000]and rapidly progressive CWP. This is defined as progression of ILO classification by greater than one sub-category over five years or less, or the development of PMF in miners exposed after 1980 [Antao et al. 2005; Blackley et al. 2014; Cohen et al. 2016]. CT is helpful for confirmation and characterization of this pattern of abnormality, and comprehensive clinical evaluation is needed to assess other potentially treatable interstitial lung diseases.

Rapidly progressive CWP has been observed in recent years in the United States, often in younger Appalachian miners [Antao et al. 2005; Blackley et al. 2014; Cohen et al. 2016]. This is thought to be due to excessive RCS exposure causing a component of accelerated silicosis. Careful comparison with prior radiographs is important to identify this clinically significant entity.

Multiple studies of coal miners show a consistent and dose-dependent relationship between exposure to respirable coal mine dust and chronic lung diseases including emphysema and chronic bronchitis [NIOSH 2011]. Coal mine dust injures the airways in an additive fashion with tobacco smoking [Kuempel et al. 2009]. All pathologic types of emphysema are associated with coal mine dust exposure, and the pathological severity of emphysema is proportional to the retained lung dust content [Green et al. 1998; Leigh 1990]. Lung function abnormalities are typically obstructive. The diffusion capacity may be decreased, and exercise-related ventilatory and gas exchange abnormalities are common.

The medical management of CMDLD consists mainly of supportive care, when appropriate. This includes interventions such as supplemental oxygen, bronchodilators, smoking cessation counseling, recommended vaccinations, weight loss, regular exercise, and pulmonary rehabilitation. Early disease recognition to minimize or eliminate ongoing coal mine dust exposure, as well as referral for appropriate benefits counseling, are both important. Lung biopsy is rarely needed to confirm chest imaging findings of CWP given an appropriate occupational exposure history.

Asbestosis and Asbestos-Related Pleural Diseases

Asbestosis is a slowly progressive fibrotic lung disease caused by inhalation of asbestos fibers. Other lung manifestations of asbestos exposure include pleural abnormalities (pleural effusions, plaques, and diffuse thickening) and chest malignancies (bronchogenic carcinoma and mesothelioma). Asbestos fibers are composed of hydrated magnesium silicates characterized by high tensile strength, weavability, and fire resistance, leading to multiple industrial uses. Exposures occur in asbestos mining and milling, industrial applications (e.g., insulation, shipbuilding, friction products, textiles), and non-occupational settings (e.g., geogenic sources, building demolition, and residential uses). Asbestos-related lung diseases typically occur with long latencies (10–30 years) following initial exposure. Insidious onset of exertional dyspnea, often with dry cough, is a usual symptom of asbestosis. Characteristic pulmonary function abnormalities may include restrictive changes, diminished diffusion capacity of the lung for carbon monoxide (D_{LCO}), and exertional hypoxemia with more advanced disease. Lung biopsy is rarely needed to confirm a diagnosis when there is a typical clinical presentation and a good exposure history.

The chest radiograph may show subtle, lower lobe predominant, small irregular opacities, often accompanied by pleural abnormalities. Many of those exposed to significant amounts of asbestos develop pleural plaques that preferentially involve the parietal pleura along the 6th through 9th ribs as well as the diaphragm (**Fig. 4**). Note the calcified and noncalcified plaque on parietal pleura (white arrows) and diaphragms (black arrows) bilaterally. Calcifications are seen in around 20% of plaques on chest radiograph and in 50% on CT. Pleural plaques and pleural thickening must be distinguished from extrapleural fat, which is characterized by relatively low attenuation soft tissue thickening, extending symmetrically in undulating fashion along the lateral chest wall all the way to the lung apices (**Fig. 5**), while pleural plaques are usually more focal and asymmetric [Sargent et al. 1984]. However, focal extrapleural fat may be impossible to distinguish on imaging from noncalcified pleural plaques but can be identified on CT. Note the attenuation of pleural thickening (black arrows) similar to subcutaneous fat (white arrow) in **Fig. 6**. Rounded atelectasis, which can occur as a consequence of asbestos-related pleural thickening or effusion, is characterized by a mass-like opacity adjacent to thickened pleura, with associated lobar volume loss, and curving of bronchi and vessels into the mass (**Fig. 7**) [Lynch et al. 1988; McHugh and Blaquiere 1989]. Benign asbestos pleural effusions are usually small and unilateral and are one of the earliest imaging manifestations of asbestos exposure. Characteristic HRCT findings of asbestosis include subpleural linear densities, interlobular septal thickening, centrilobular thickening, subpleural parenchymal curvilinear opacities (**Fig. 8**), reticular opacity with traction bronchiectasis and honeycombing in severe disease similar in appearance to usual interstitial pneumonia (UIP).

As with the other pneumoconioses, there is no proven safe and effective specific treatment for asbestosis. Management includes early disease detection and removal from exposure, supplemental oxygen for hypoxia, prompt treatment of any lung infection, and appropriate vaccinations. It also includes smoking cessation, when applicable (in part to diminish the synergistic effect of combined smoking and asbestos exposure on risk for lung malignancy).

Granulomatous Diseases

Hypersensitivity Pneumonitis

Hypersensitivity pneumonitis (HP), called extrinsic allergic alveolitis in some countries, is caused by inhalation of antigens that trigger a diffuse mononuclear cell inflammation of the small airways and lung parenchyma. The three broad categories of causal antigens are (1) fungal and microbial agents, (2) animal proteins, and (3) low molecular weight chemicals.

The clinical presentation of HP can be classified as acute, subacute, or chronic. The flu-like respiratory illness of acute HP occurs within 4 to 12 hours of exposure, with fever, cough, dyspnea, chills, malaise, chest tightness, and myalgias. Physical examination may show fever, tachypnea, tachycardia, and rales. With subacute and chronic HP, patients report the insidious onset of dyspnea on exertion, dry or minimally productive cough, fatigue, malaise, anorexia, and weight loss.
Bibasilar crackles may be detectable on lung auscultation. Right heart failure and digital clubbing may be present in advanced cases of fibrosis. Pulmonary function testing shows restriction, obstruction, or mixed abnormalities, often with decreased D_{LCO} or exercise-induced gas exchange abnormalities.

The chest radiograph (CXR) is often normal in patients with HP (**Fig. 9**), with an estimated sensitivity of only 10% [Hodgson et al. 1989]. In acute HP, the CXR may show diffuse ground glass or airspace consolidation. Patients with subacute HP may have a combination of nodular or reticulonodular opacities with ground glass. Chronic fibrotic HP usually has a CXR appearance of reticular opacities with honeycombing. Though the HRCT pattern is variable depending on the stage of HP, characteristic findings include centrilobular ground-glass nodular opacities, diffuse ground-glass abnormality, and mosaic attenuation (**Fig. 9**)**,** hypersensitivity pneumonitis showing features of ground glass opacity, nodularity, and mosaic attenuation). **Figure 10** shows the evolution of chronic hypersensitivity pneumonitis from ground-glass opacity to fibrosis. Such findings may be seen in patients with acute, subacute, or chronic disease. The distribution of findings in acute or subacute HP is often diffuse, while the findings of chronic HP may show upper, middle, or lower lung predominance [Silva et al. 2008]. Some patients with chronic HP develop lung fibrosis, characterized by reticular abnormality, traction bronchiectasis, and sometimes honeycombing with cystic changes and often is associated with centrilobular nodularity, ground glass, or mosaic attenuation (**Fig. 11**). Emphysema (**Fig. 12**) may also occur in chronic HP, even in never-smokers.

Histologic findings vary depending on the stage of the disease. The classic HP triad of histopathologic features is lymphocytic alveolitis; small, loose non-necrotizing granulomas; and cellular bronchiolitis. In chronic HP, variable stages of interstitial fibrosis may be found including a nonspecific interstitial pneumonitis (NSIP) pattern, centrilobular and peribronchiolar fibrosis, bridging fibrosis, and a UIP-like pattern. Findings of lymphocytic infiltration, giant cells, poorly formed granulomas, and bridging fibrosis can help differentiate HP from other fibrotic lung diseases.

Chronic Beryllium Disease

Chronic beryllium disease (CBD) is an immune-mediated granulomatous lung disease resembling sarcoidosis that is caused by exposure to the lightweight metal beryllium. Exposure can occur in several industries including aerospace, defense, metal machining, electronics manufacture and recycling, and dental alloy/appliance production. Diagnosis requires a history of beryllium exposure, a positive blood or bronchoalveolar lavage (BAL) beryllium lymphocyte proliferation test (BeLPT), and noncaseating granulomas or mononuclear cell infiltrates on lung biopsy. A patient is considered beryllium-sensitized when the patient has a positive blood BeLPT but no abnormal lung pathology. When histopathology is unavailable, a CBD diagnosis can be made based on the exposure history, a positive BeLPT, and imaging that shows abnormalities consistent with CBD. In early CBD, pulmonary function abnormalities, if present, include mild airflow limitation and abnormal gas exchange at rest or with exercise. Diffusing capacity (D_{LCO}) may be low, and arterial blood gas analysis with exercise may show gas exchange abnormalities. With more advanced disease, pulmonary function tests (PFTs) show airflow limitation, restriction, or a mixed pattern.

In early disease, the chest radiograph may be normal or show hilar adenopathy or parenchymal abnormalities. Parenchymal abnormalities include nodules, ground glass,
linear or alveolar opacities. The parenchymal abnormalities may be diffuse or upper lobe predominant. HRCT is more sensitive than chest x-ray in diagnosing CBD; however, HRCT is normal in up to 25% of patients with biopsy-proven CBD [Newman et al. 1994]. HRCT findings of CBD include parenchymal nodules of varying size, thickened septal lines, ground glass opacities, cystic cavitation, bronchial wall thickening, and hilar/mediastinal adenopathy [Naccache et al. 2003; Newman et al. 1994].

The lack of effective treatment, the progressive nature of the disease with ongoing exposure, and the severity of fixed obstruction often seen in affected workers underscore the need for early recognition and control of causal exposures.

Chest radiographs are generally normal in early disease stages but may show hyperinflation. Characteristic findings on HRCT include segmental or lobular areas of low attenuation associated with narrowing of pulmonary vessels (mosaic perfusion) (**Fig. 13**).

The Central Role of Diagnostic Imaging

Imaging is critical in the early detection of occupational lung disease, both on the chest radiograph and on HRCT. Early detection of occupational lung disease changes requires awareness of the variety of patterns that may occur in these diseases. The ILO classification focuses on small round opacities (nodules) and small irregular opacities (reticular pattern) because these are the most frequent patterns found in classic pneumoconioses. The emphasis on these important patterns should not lead the interpreter to ignore other abnormalities potentially related to occupational exposures, including ground glass abnormality, consolidation, airway wall thickening, and emphysema (**Table 1**). The image interpreter must also be aware of potential non-occupational causes of these patterns, as shown in **Table 1**, and include these non-occupational entities in the differential diagnosis of radiologic abnormalities.

Table 1: Radiologic patterns of lung disease associated with occupational exposures on chest radiograph and chest CT.

Pattern	**Common occupational diseases or exposures**	**Differential diagnosis**
Small rounded opacities	Coal worker's pneumoconiosis Silicosis Other pneumoconioses (talcosis, stannosis, etc.) Chronic beryllium disease	Sarcoidosis Chronic mycobacterial (e.g., miliary tuberculosis) or fungal infection
Large opacities	Coal worker's pneumoconiosis Silicosis Chronic beryllium disease	Sarcoidosis, malignancy (if unilateral) Chronic mycobacterial or fungal infection
Small irregular opacities (reticular or linear)	Asbestosis Coal worker's pneumoconiosis Silicosis Chronic hypersensitivity pneumonitis	Idiopathic interstitial pneumonias (nonspecific interstitial pneumonia, usual interstitial pneumonia) Collagen vascular disease Smoking-related lung disease Lymphangitic carcinomatosis
Ground-glass opacity	Hypersensitivity pneumonitis Acute or subacute inhalational lung injury Hard metal pneumoconiosis Chronic beryllium disease	Smoking-related lung disease Drug toxicity Pulmonary hemorrhage Aspiration
Consolidation	Acute or accelerated silicosis Acute or subacute lung injury	Infection Pulmonary hemorrhage Malignancy Organizing pneumonia Aspiration
Bronchial wall thickening	Acute or subacute toxic fume Inhalation Occupational bronchitis Occupational asthma	Bronchitis Asthma
Emphysema	Silicosis Coal worker's pneumoconiosis Hypersensitivity pneumonitis	Smoking-related lung disease Alpha-1 antitrypsin deficiency
Mosaic attenuation/air trapping	Bronchiolitis from toxic fume or chemical inhalation (e.g., flavoring chemicals)	Obliterative bronchiolitis related to collagen vascular disease, previous infection, etc.
Pleural thickening/plaques	Asbestosis	Infection, trauma, neoplasm

Digital Radiography

Since the United States and most other countries have transitioned from analog to digital chest radiographs, it is increasingly difficult to obtain good quality analog chest radiographs in many locations. Advantages of digital radiography include availability of multiple identical copies of images and potential for remote reading. Potential disadvantages include the requirement for high quality monitors for image viewing and difficulty in standardizing algorithms for image acquisition and reconstruction. For these reasons, the ILO published the 2022 new digital standard radiographs for use in pneumoconiosis classification of digital radiographs [ILO 2023]. Digital radiographs should always be classified based on side by side comparison with these standard images. NIOSH has published detailed specifications for acquisition and processing of digital images [HHS 2012]. Additionally, NIOSH offers dedicated free software (NIOSH BViewer©) to facilitate radiographic classification and comparison between worker/patient images and reference standard images.

Role of CT

The chest radiograph remains important in detection and characterization of occupational lung disease because of its relatively low cost, relatively low radiation dose, and wide availability. However, the chest radiograph is relatively insensitive to early interstitial abnormality, and imprecise for evaluation and characterization of parenchymal and pleural disease. For these reasons, interest is increasing in the use of CT in the diagnosis of occupational lung diseases, particularly in specific contexts as delineated below. Optimal HRCT technique to detect occupational lung disease includes contiguous thin sections (1.5 mm or less), acquired during suspended deep inspiration, with high resolution reconstruction [Mayo 2009]. Coronal and sagittal reconstructions from volumetric acquisitions are frequently useful, as shown in several illustrations in this section. Prone images are often helpful to identify early fibrosis in the posterior lungs, and expiratory images are helpful to identify air trapping.

Detection of Early Pneumoconiosis

HRCT is generally more sensitive than chest radiographs for detecting early dust diseases of all types, particularly in workers with normal or 0/1 profusion chest radiographs [Akira et al. 1989; Bergin et al. 1986; Huuskonen et al. 2001; Staples et al. 1989]. In subjects with asbestos exposure who have chest radiograph profusion scores of 0/1 or 1/0, the presence of fibrosis on HRCT (**Fig. 8**) has been shown to identify subjects with abnormal physiology and bronchoalveolar lavage findings suggestive of asbestosis, while those with normal HRCT generally have normal physiology and bronchoalveolar lavage [Harkin et al. 1996]. Conversely, chest radiographs may be false positive, and HRCT may fail to confirm pneumoconiosis, indicating that there may be false positive chest radiographs [Remy-Jardin et al. 1990]. **Figure 14** demonstrates pleural thickening at left base on chest radiograph. The CT image shows pleural plaque not visible on the chest radiograph. Additionally, HRCT has been recognized as more sensitive for detecting coalescent and conglomerate large opacities compared to radiographs [Remy-Jardin et al. 1990]. HRCT is also superior to chest radiograph in detecting emphysema and other airway effects of dust exposure [Erkinjuntti et al. 1990].

Detection of Pleural Disease

Several papers demonstrate that CT is more sensitive and more specific than chest radiographs for asbestos-related pleural disease [Aberle et al. 1988a,b; Gevenois et al. 1998]. In particular, CT can identify non-calcified face-on pleural plaques, and readily distinguish pleural plaque from extrapleural fat, a frequent cause of overdiagnosis of pleural disease on the chest radiograph [Ameille et al. 1993]. (**Fig. 5**), (**Fig. 6**). Additionally, CT helps identify subjects with round atelectasis related to diffuse pleural thickening, which is often associated with restrictive physiology and must be distinguished from malignancy (**Fig. 7**) [Lynch et al. 1988; McHugh and Blaquiere 1989].

Screening for Malignancy

The landmark National Lung Cancer Screening Trial demonstrated a 20% reduction in mortality from lung cancer in heavy smokers who underwent annual CT screening for 3 years, compared with a control group screened with annual chest radiographs [The National Lung Screening Trial Research Team 2011].

The United States Preventive Services Task Force (USPSTF) therefore recommends annual screening for lung cancer with low-dose CT in adults aged 50 to 80 years who have a ≥20 pack-year smoking history and currently smoke or have quit within the past 15 years [US Preventive Services Task Force 2021]. A substantial number of occupational exposures, including asbestos, arsenic, beryllium, cadmium, nickel, radon, and silica, cause lung cancer [Gottschall 2002]. The role of CT in screening for occupational-related malignancy in those who do not meet the USPSTF guidelines remains unclear. Patients with occupational exposures who are screened with CT should be carefully evaluated for evidence of both non-malignant and malignant occupational lung disease.

Identifying Non-Pneumoconiotic Occupational Lung Diseases

As shown in **Table 1**, non-pneumoconiotic occupational lung diseases are often associated with findings that are subtle, nonspecific, or not visible on chest radiographs. For example, many cases of hypersensitivity pneumonitis are characterized by ground glass abnormality, which is easy to identify on HRCT but difficult to see on chest radiograph [Lynch et al. 1992]. Similarly, obliterative bronchiolitis related to inhalational exposure is difficult to identify on chest radiograph. HRCT with inspiratory and expiratory views that would permit identification of air trapping may be very helpful in symptomatic patients with known occupational exposures who have normal or near-normal chest radiographs.

Systematic Scoring of Occupational Lung Disease on HRCT

A standardized system for scoring extent of disease on HRCT, very similar to the ILO radiographic classification system, has been published [Kusaka et al. 2005] and is widely used [Hering 1992; Hering et al. 2004; Kraus et al. 2009; Suganuma et al. 2006; Tamura et al. 2015]. This system has been associated with moderate inter-reader and intra-reader agreement for all categories of abnormality except ground glass opacity [Huuskonen et al. 2001].

Overview of Non-imaging Clinical Tools in Lung Disease Diagnosis

Occupational and Environmental Exposure History: The Key to Diagnosis

A detailed medical and exposure history remains the mainstay of diagnosing occupational and environmental lung diseases. The three essential components of a comprehensive occupational history are (1) a chronology of current and previous jobs, (2) a detailed description of current and previous job duties, tasks, and exposures, and (3) questions about symptom onset, timing, and duration in relation to workplace exposures.

Information on non-occupational exposures should also be elicited, particularly those in the home or with recreational and avocational activities. A complete medical history is important in assuring that co-factors with and confounders of occupational exposures, such as tobacco use, heart disease, and non-occupational lung diseases, have been considered in the diagnostic assessment.

Physical Examination and Laboratory Studies

As with most lung diseases, findings on lung examination are often normal or nonspecific and typically occur late in the course of disease. Wheezing may be a sign of airway obstruction. End-inspiratory squeaks or snaps have been associated with bronchiolitis. End-inspiratory crackles suggest later stages of fibrotic interstitial lung disease. Digital clubbing is a sign of end stage illness and reflects a poor prognosis. Lower extremity edema can occur with either right or left heart failure and may signal chronic hypoxemia with cor pulmonale.

Serologic markers can help distinguish occupational lung diseases from other conditions and may help determine a specific diagnosis. A positive blood BeLPT distinguishes chronic beryllium disease from sarcoidosis. Though autoimmune interstitial lung diseases are often on the list of differential diagnoses when evaluating a patient with lung disease, positive autoimmune serologies can be seen in several pneumoconioses. In patients with silicosis, autoimmune serologies, including positive rheumatoid factor (RF) and anti-nuclear antibodies, may accompany silica-related nephritis.

Pulmonary Function Testing (Resting PFTs, Cardiopulmonary Exercise Testing, Inhalation Challenge)

Resting PFTs are essential tools used to diagnose some occupational lung diseases and measure the severity of impairment, and response to treatment. Resting pulmonary function abnormalities may be obstructive, restrictive, or mixed, depending on exposures and host factors. Cardiopulmonary exercise testing is often useful to evaluate impairment and assess the presence and severity of gas exchange abnormalities. Methacholine challenge testing to assess the presence and severity of airway hyper-responsiveness is useful in the assessment of suspected occupational asthma.

Bronchoscopy and Surgical Lung Biopsy

For most occupational lung diseases, a careful occupational and environmental exposure history, in combination with non-invasive clinical testing, is adequate for diagnosis. Occasionally, however, fiberoptic bronchoscopy with bronchoalveolar lavage (BAL) and transbronchial biopsies may be clinically indicated. This is particularly true for granulomatous lung diseases, where finding a lymphocytic alveolitis can help confirm a diagnosis of HP or when a positive BAL BeLPT is essential for diagnosing CBD. For fibrotic interstitial lung diseases (ILDs) and in some cases of presumptive occupational bronchiolitis, surgical lung biopsy may be important in confirming a diagnosis and in deciding whether systemic therapy (i.e., oral corticosteroids or immunosuppressive agents) is warranted. With the availability of newer treatment modalities for UIP or idiopathic pulmonary fibrosis (IPF), histologic confirmation and differentiation from similar occupational ILDs may be clinically important.

Conclusions

Diagnosing an occupational lung disease is based on a combination of findings from history and physiological and radiological assessment. Complete occupational and environmental exposure histories, along with information on potential confounding factors such as smoking and co-morbid conditions, are essential to diagnosis and management. When considering occupational interstitial lung diseases, the importance of imaging for diagnosis is unequivocal. Specific treatment for many occupational lung diseases is limited or unavailable, particularly for pneumoconioses. In addition to supportive medical management, care of the affected patient may require complete exposure cessation and referral for benefits counseling. Integration of imaging findings (including judicious use of HRCT) with other findings on clinical evaluation is important to achieve diagnostic accuracy, facilitate early disease detection, and optimize long-term care and prevention.

Appendix A

Occupational lung diseases that do not usually require chest imaging with ILO classification for surveillance or diagnosis.

Airway Diseases

Occupational Asthma

One of the most common occupational lung diseases, occupational asthma (OA) is characterized by variable airflow obstruction, airway hyper-responsiveness, and airway inflammation from workplace exposures. The two main types are (1) OA occurring after a period of latency with ongoing immunologic exposure, and (2) OA from non-immunologic exposures, often following a single exposure to a high concentration of a known irritant (e.g., chlorine or related compounds). Work-aggravated asthma is defined as pre-existing asthma that is exacerbated by workplace exposures such as secondhand smoke or extremes of temperature and humidity. Common immunologic exposures that can cause OA include low molecular weight chemicals (most commonly, isocyanates used in paints and foams, as well as wood dusts, acrylates, and some metals such as platinum, nickel, cobalt, and chromium) and high molecular weight (HMW) substances (e.g., latex, laboratory and farm animals, pharmaceutical agents, baking and detergent enzymes).

Typical symptoms of OA include cough, sputum production, wheezing, chest tightness, and dyspnea. Pulmonary function testing to confirm the diagnosis of asthma may show airflow obstruction (FEV1/FVC ratio below the lower limit of normal) with significant improvement following bronchodilator (defined as a 10% improvement in the percent reference of FEV1 or FVC). If airflow obstruction is not present on spirometry, a methacholine challenge may be necessary to determine the presence and severity of bronchial hyper-responsiveness. Serial measurement of peak expiratory flow rates (PEFR) at and away from work is sometimes helpful. Skin prick testing or immunoassays for specific IgE (Immunoglobulin E) using extracts of HMW substances may aid diagnosis in some circumstances. The chest radiograph in OA may be normal or show hyperinflation. HRCT is usually unnecessary for evaluating suspected OA unless an abnormality is noted on the chest radiograph, or if there is a concern for another disease, such as hypersensitivity pneumonitis.

Emphysema and Chronic Bronchitis

Chronic obstructive pulmonary disease (COPD) is the most common chronic lung disease in developed countries, affecting 5%–10% of the population. Lung function testing typically shows airflow limitation (reduced ratio of FEV1 to FVC) that is not fully reversible, often accompanied by air trapping based on an elevated residual volume and decreased diffusion capacity for carbon monoxide. Though cigarette smoking is the most common cause of COPD, it is now recognized that COPD occurs in non-smokers and that cigarette smoking accounts for only 50%–70% of the variation in COPD prevalence found in epidemiological studies. Multiple studies from over 30 countries show a population-attributable fraction for COPD of 15%–20% of workplace exposures [American Thoracic Society 2003; Eisner et al. 2010]. COPD caused by occupational exposures has no clinical or pathophysiological features that distinguish it from non-occupational COPD. COPD from any cause is characterized histologically by the destruction of alveolar walls (emphysema) with epithelial thickening and peri-bronchiolar fibrosis and a reduction in the number of small airways.

Several specific industries and exposures have been linked to increased COPD risk. Cross-sectional and longitudinal studies show that cumulative exposure to coal mine dust is associated with an accelerated decline in FEV1, and the effect of coal mine dust exposure is similar to that of cigarette smoking [Rogan et al. 1973]. Autopsy studies of coal miners show relationships between lifetime coal mine dust, post-mortem lung dust content, and the presence and severity of emphysema [Kuempel et al. 2009]. Elevated standardized mortality ratios for COPD have been reported in silica-exposed workers, with some studies showing exposure-response relationships [Hnizdo et al. 1991, 2000; Kreuzer et al. 2013]. Other reported causes of occupational COPD or emphysema include metals (cadmium, aluminum, beryllium, and cobalt); other inorganic dusts (carbon black, potash); specific fume and gas exposures (welding fumes, diesel exhaust, coke oven emissions, and chlorine and sulfur dioxide exposures in paper and pulp mill workers); organic dusts (in animal farming, cotton processing, silk, and hemp workers, and those exposed to wood dusts); and hypersensitivity pneumonitis (**Fig. 12**) [Erkinjuntti-Pekkanen et al. 1998]. Studies examining more general occupational exposures to vapor, gas, dust, and fumes (VGDF) have shown that such exposures are associated with risk for COPD and indicate the public health importance of these workplace exposures on COPD disease burden [Harber et al. 2007].

Occupational Bronchiolitis

Small airways of less than 2 mm in diameter—both membranous and respiratory bronchioles—may be affected by workplace inhalational exposures. The pathogenesis of occupational bronchiolitis likely involves injury to the bronchiolar epithelium, followed by excessive proliferation of granulation tissue during the repair process. This leads to concentric narrowing (constrictive bronchiolitis) or obliteration (obliterative bronchiolitis) of the airway lumen. Acute, high-dose inhalational exposures to several toxic workplace agents—classically the oxides of nitrogen and sulfur—are associated with acute or subacute obliterative bronchiolitis, often with organizing pneumonia. More insidious onset of work-related bronchiolitis has been linked with exposure to diacetyl and other chemicals used in the manufacture of artificial flavorings. Workers producing microwave popcorn, as well as flavor production and upstream flavor chemical manufacturing workers, may be at risk [CDC 2007]. Military personnel deployed to Iraq and Afghanistan may develop subacute bronchiolitis, though the causal agent or agents is uncertain [King et al. 2011]. Fiberglass boat builders working with styrene and other chemicals used in glass-reinforced plastics may develop rapidly progressive obliterative bronchiolitis [Cullinan et al. 2013]. Diagnosis of occupational bronchiolitis requires a high index of suspicion, as clinical findings are often nonspecific. A work-related pattern of respiratory symptoms is generally lacking in the subacute and chronic forms. Accelerated decline in FEV1 may be seen, often with an elevated residual lung volume and normal diffusion capacity.

Pathology Overview

The Pathology Basis of Occupational Lung Disease

Introduction

Tissue pathology is the standard upon which the radiographic recognition of pneumoconiotic lesions has historically been derived. It follows, therefore, that knowledge of morphology helps to place radiologic findings into pathologic and clinical perspectives, may improve diagnostic acumen, and lends credibility to the interpretation of radiologic images. The spectrum of pneumoconioses encompasses a variety of injurious minerals inhaled in various occupational settings, and the patterns of lung remodeling differ with the inhaled agent (or agents), the intensity and duration of exposure, and mitigating intrinsic or extrinsic factors that affect tissue reaction or dust removal from the lung. Regardless of the inciting mineral, certain basic lesions characterize diverse disease entities and impart similar appearances in the chest radiograph. The three classic disorders encompass most pneumoconiosis cases encountered radiologically: CWP, silicosis, and asbestos-related pleuropulmonary disease. Understanding the pathology of these three entities serves as a foundation for radiologic interpretation of the pneumoconioses and owing to the stereotyped responses of the lung to injury, is relevant for assessing radiologic changes in less frequent types of mineral dust exposures.

Pulmonary Silicosis

Pulmonary silicosis is caused by inhaling free respirable crystalline silica (RCS). It is important to distinguish between silica (i.e., silicon dioxide) and silicates, in which silicon is combined with various cations and anions in a crystalline matrix. Silicates, including asbestos, are common in the industrial setting. They are generally less fibrogenic than RCS, and, when present in combination with silica, may alter the tissue reaction, producing a mixed-dust fibrotic nodule [Craighead et al. 1988].

Nodular Silicosis

The anatomic hallmark of pulmonary silicosis is the silicotic nodule, a well-demarcated, rounded fibrotic lesion that tends to concentrate in the upper lung lobes. Macroscopically, nodules range from gray to black depending on the amount of associated carbonaceous dust or other black pigments incorporated into the lesion. In its mature form, the silicotic nodule is microscopically composed of concentrically arranged coarse collagen bundles of low cellularity (**Fig. 15**). In younger lesions, the central fibrotic core is cuffed by a rim of fibroblasts and dust-laden macrophages. Cellular nodules composed of histiocytes, resembling granulomas, are a notable feature of accelerated silicosis due to very heavy silica exposure [Craighead et al. 1988; Gibbs and Wagner 1998]. Under polarized light microscopy, silica can be recognized within the nodules as weakly birefringent polyhedral particles approximately 1 to 2 microns in maximal dimension, typically interspersed with black pigment and brightly birefringent needle-like silicate crystals (**Fig. 16**).

Focal calcification and central necrosis and breakdown are variable features of silicotic nodules. Nodular pulmonary silicosis is classified pathologically as small opacity disease (sometimes called simple) or complicated (PMF), according to the size of the nodules. Large radiographic opacities greater than 1 cm in long axis diameter are designated as PMF. The minimum size criterion for diagnosing complicated silicotic nodules has also been generally agreed to be greater than 1 cm in long axis diameter [Craighead et al. 1988; Gibbs and Wagner 1998]. Growth of silicotic nodules may occur by expansion of individual lesions or more often by fusion of multiple nodules, forming a conglomerate nodule (Fig. 15). Thus, PMF (complicated silicosis) occurs in a background of small opacity silicosis. Large silicotic nodules may be associated with paracicatricial emphysema with or without emphysematous bullae. As they enlarge, conglomerate lesions not only replace lung parenchyma but also may cross interlobar fissures and obliterate pulmonary arteries, leading to pulmonary hypertension. Ischemia of large nodules may result in central necrosis and cavitation. Inhalational silica exposure also increases the risk for mycobacterial infections. Consequently, mycobacterial granulomas can modify the morphology of silicotic nodules, introducing Langhans giant cells, caseation necrosis, cavitation, and acid-fast bacilli into the histological picture.

Mixed-Dust Fibrosis

In some industrial settings, such as foundry work or coal mining, inhaling RCS with other minerals leads to a characteristic stellate nodule of mixed-dust fibrosis. The stellate nodule, as opposed to the more classical rounded silicotic nodule, has irregular extensions into the adjacent lung parenchyma, producing a “Medusa-head” lesion (Fig. 17). Abundant black pigment and brightly birefringent silicate particles impregnate stellate nodules. Since a mixture of nonsiliceous minerals or black pigment is often associated with classical silicosis, the determinants for developing mixed-dust fibrotic nodules are somewhat uncertain [Craighead et al. 1988].

Acute and Accelerated Silicosis

Acute silicosis is characterized pathologically by the filling of alveolar spaces by lipoproteinaceous material that stains red-violet with periodic acid–Schiff stain (Fig. 18). There may be associated diffuse alveolar septal fibrosis and small, cellular, poorly formed silicotic nodules [Buechner and Ansari 1969; Craighead et al. 1988]. In acute silicosis, silica particles may be difficult to visualize with polarized light because of their exceedingly small size. Accelerated silicosis is also a severe progressive form of silicosis caused by inhalation of abundant fine silica particles. The time course of accelerated silicosis is intermediate in duration between acute and chronic silicosis. Cellular silicotic nodules may resemble granulomas in the early stages, with progression to massive conglomerate fibrosis in the later stages of the disease.

Lymph Node Silicosis

Lymph node involvement by silicotic nodules frequently accompanies pulmonary silicosis and is often an isolated finding in exposed individuals with no radiologic or histologic stigmata of pulmonary silicosis. The morphology of nodules in lymph nodes is identical to those in the lung parenchyma. Extension of lesions beyond the capsule of the lymph node into the lung hilum can result in hilar fibrosis and bronchial stenosis. Peripheral calcification of silicotic lymph nodes may produce the classical radiographic appearance of “eggshell calcification” in approximately 10% of cases [Craighead et al. 1988]. Erosion of calcified lymph nodes into adjacent airways is an infrequent cause of obstructive broncholithiasis [Cahill et al. 1992].

Coal Workers’ Pneumoconiosis

Coal workers’ pneumoconiosis is defined as parenchymal lung disease secondary to inhaling coal mine dust, which includes both carbonaceous (coal) and noncarbonaceous minerals such as silica and silicates. The composition of coal mine dust and the severity of exposure varies with the miner’s job description [Green and Vallyathan 1998; Kleinerman et al.1979]. Like silicosis, CWP is classified as small opacity or PMF (complicated) depending on the size of individual lesions. A comprehensive review of the pathology of CWP has recently been published [Cool et al. 2023].

Small Opacity CWP

Inhaled coal particles within the lung are coarse, irregular, often angulated, and black (Fig. 19). The earliest and most distinctive lesion of simple CWP is the coal macule. On macroscopic examination, coal macules appear as barely palpable (or nonpalpable) darkly pigmented foci, ranging in size from approximately 1 to 5 mm (Fig. 20). Microscopically, macules are formed by the deposition of black pigment, with minimal associated fibrosis within and around the walls of respiratory bronchioles and alveolar ducts. Airspace dilatation around the macule, termed *focal emphysema*, is an integral component of the lesion and is considered to represent a form of centrilobular emphysema (Fig. 21) [Green and Vallyathan 1998; Kleinerman et al. 1979]. Simple CWP may also include the presence of small, heavily pigmented, fibrotic nodular lesions of two morphological forms: stellate lesions of mixed-dust fibrosis (Fig. 17) or rounded nodules resembling silicotic nodules (Fig. 22). The formation of fibrotic nodules is thought to be related to the content of silica in inhaled coal mine dust [Green and Vallyathan 1998].

CWP with Progressive Massive Fibrosis (Complicated CWP)

Progressive massive fibrosis in CWP (complicated CWP) bears similarities to PMF in silicosis (complicated silicosis) because of fibrotic nodules appearing as large opacities that are greater than one cm in long axis diameter on chest imaging. The minimum size criterion for the diagnosis of complicated silicotic nodules has also been generally agreed to be greater than 1 cm in long axis diameter [Cool et al. 2023; Green and Vallyathan 1998; Kleinerman et al.1979].

Lesions of PMF usually occur on a background of small opacity CWP and are upper lobe predominant; however, lesions have been described in the middle and lower lung zones [Halldin et al. 2020]. Macroscopically, lesions of PMF are heavily pigmented, destructive fibrous nodules that may transgress interlobar fissures (Fig. 23). Compared with PMF in silicosis, the nodular lesions of PMF in CWP tend to have more abundant black pigment, fewer birefringent crystals, and irregular borders. However, with heavy silica exposure, nodules may be more rounded because of coalescence of silicotic-type fibrohyaline nodules. Paracicatricial emphysema with or without bullae commonly surrounds large PMF lesions. PMF lesions may exhibit central ischemic necrosis and cavitation. Microscopically, PMF lesions are composed of coarse collagen bundles arranged in a haphazard manner, interspersed with black pigment (Fig. 24).

There has been recent documentation of a severe variant of CWP characterized by accelerated decline in lung function and rapid radiographic CWP progression among U.S. coal miners [Petsonk et al. 2013]. This is thought to be due to excessive respirable crystalline silica exposure causing a component of accelerated silicosis. Pathologic findings in a subset of miners with rapidly progressive pneumoconiosis showed PMF in the majority with features of silicosis and mixed-dust lesions, associated with large amounts of birefringent mineral dust particles consistent with silica and silicates. A minority of cases have been characterized pathologically as dust-related diffuse fibrosis or DDF [Cohen et al. 2016].

Rheumatoid Pneumoconiosis (Caplan Syndrome)

Rheumatoid pneumoconiosis represents a form of pneumoconiosis affecting coal miners (and other mineral dust-exposed individuals) who also have rheumatoid arthritis or serological evidence of rheumatoid factor [Green and Vallyathan 1998]. Rapidly developing nodules of variable size appear macroscopically like giant silicotic nodules but have a softer texture and often a laminated appearance. Thin-walled cavities like the necrobiotic nodules seen with rheumatoid arthritis may also occur (Fig. 25). Background simple CWP is frequently of a mild degree [Gough et al. 1955]. The histological features of Caplan nodules include laminated black pigment with central necrosis, cavitation, eosinophilic degeneration of collagen, and palisaded histiocytes or chronic inflammation around the necrotic zone (Fig. 26). Caplan nodules must be distinguished from mycobacterial lesions. Evaluation for mycobacteria and other infectious organisms is required for any necrotic or cavitated lesion of CWP, even when granulomatous inflammation is absent.

Associated Lesions: Emphysema and Diffuse Interstitial Fibrosis

Inhalation of coal mine dust has been determined to be an independent risk factor in the development of emphysema [Cockcroft et al. 1982; Green and Vallyathan 1998; Ruckley et al. 1984b]. Progressive centrilobular emphysema constitutes an extension of focal emphysema associated with the coal macule. Panacinar emphysema represents a less common variant associated with coal dust exposure.

In a study that evaluated emphysema severity in whole-lung thick sections from autopsies of 722 U.S. coal miners performed from 1957 to 1973, Kuempel et al. [2009] found that emphysema was significantly elevated in coal miners compared with non-miners and among ever and never-smokers, and that cumulative exposure to respirable coal mine dust and coal dust retained in the lungs were significant predictors of emphysema severity [Kuempel et al. 2009].

Pulmonary interstitial fibrosis documented at autopsy has been variably reported in the lungs of coal miners in as many as 33% of cases. Interstitial fibrosis may macroscopically resemble honeycomb lung. Histologically, black pigment and mineral deposition in the areas of interstitial fibrosis were noted in 53% of cases (Fig. 27). However, in the remaining 47%, interstitial fibrosis was nonpigmented, resembling the type of fibrosis seen in idiopathic pulmonary fibrosis [McConnochie et al. 1988]. Chronic interstitial pneumonia and fibrosis resembling usual interstitial pneumonia were also identified in a subset of French coal miners with clinical and radiologic evidence of interstitial lung disease with honeycombing [Brichet et al. 2002].

Asbestosis

Unlike the compact mineral particles of silica and coal mine dust, asbestos represents a family of fibrous silicates presenting as thin filaments with a high aspect (length to width) ratio. The two mineralogic forms of asbestos are amphiboles (e.g., crocidolite and amosite) and serpentines, of which chrysotile is the only commercially important form. Although restrictions have been placed on the use of asbestos in developed countries, asbestos exposure still remains an important cause of lung and pleural disease in persons previously exposed to airborne asbestos fibers and in those who continue to be exposed in the processing, application, or removal of asbestos or its products [American Thoracic Society 2004].

Because of their irregular or long filamentous configurations, asbestos fibers tend to be deposited at the bifurcation of small airways and subsequently pass into and through bronchiolar walls. Smaller fibers reach the lung parenchyma via the airstream, where they can penetrate alveolar septa or the visceral pleura [Churg 1998b]. Amphibole asbestos is durable within the lung, whereas chrysotile degrades over time because of the leaching of magnesium ions. Short asbestos fibers may be phagocytized by alveolar macrophages and subsequently removed from the lung by means of airways or lymphatics [Churg 1998b]. A relatively minor proportion of larger fibers are coated with protein and iron by alveolar macrophages to form asbestos bodies [Roggli 2004]. Unlike uncoated fibers, asbestos bodies can be readily recognized by light microscopy in slides of lung tissue and serve as valuable markers of asbestos exposure (Fig. 28). Histochemical stains for iron enhance the recognition and detection of asbestos bodies in tissue. Asbestos is fibrogenic to the lung and pleura, is a recognized cause of lung carcinoma, and is the most important cause of pleural mesothelioma [Roggli et al. 2010].

Asbestosis is defined as lung parenchymal fibrosis due to inhaled asbestos fibers [American Thoracic Society 2004; Churg 1998b; Roggli et al. 2010]. Macroscopically, the lung is remodeled by interstitial fibrosis and honeycombing, frequently with a lower-lobe distribution, imparting an appearance similar to that of idiopathic pulmonary fibrosis. Coarse gray fibrous trabeculae and fibrotic interlobular septa extend into the lung parenchyma, which often has a bronze discoloration in the fixed specimen (Fig. 29). Histologically, the extent (and progression) of fibrosis is graded from 1 (fibrosis confined to the walls of respiratory bronchioles and the first tier of adjacent alveoli) to 4 (honeycomb changes) [Roggli

et al. 2010]. Fibrosis histologically has a chronic collagenous appearance with low cellularity and irregular effacement of alveolar architecture, which gives rise to small irregular opacities in the chest radiograph (**Fig. 30**) [Dick et al. 1992]. Two or more asbestos bodies per square centimeter of a 5 mm-thick lung section, in combination with interstitial fibrosis of the appropriate pattern, are indicative of asbestosis (**Fig. 28**). Fewer asbestos bodies do not necessarily exclude a diagnosis of asbestosis, but evidence of excess asbestos would then require quantitating fibers by electron microscopy following lung digestion and sediment extraction [Roggli and Sharma 2004; Roggli et al. 2010].

Asbestos-Induced Benign Pleural Disease

Asbestos has a predilection for pleural injury, although the precise pathogenetic mechanisms by which fibers are deposited in the pleura and induce pleural changes are unclear [Oury 2004]. The nonneoplastic pleural disorders ascribed to asbestos include benign pleural effusion, plaques, and diffuse pleural fibrosis. Unexplained pleural effusions due to asbestos occur and may precede subsequent asbestos-related pleural disease. The histological changes in the pleura associated with asbestos-induced effusion have not been extensively documented, but chronic pleuritis with organizing fibrin may be seen. The pleural fluid is exudative and either serous or serosanguineous with leukocytosis. The diagnosis of asbestos-related pleural effusion is one of exclusion and requires extended follow-up to rule out malignancy. Chronic effusions may lead to diffuse pleural fibrosis [Gaensler and Kaplan 1971; McLoud et al. 1985].

Pleural plaques constitute an important marker of asbestos exposure. Plaques are defined as discrete, elevated, circumscribed fibrotic lesions usually located on the parietal pleura [Oury 2004]. Macroscopically, plaques are pearly white, rubbery, or hard because of calcification, with scalloped edges. The shape varies from flat and discoid to nodular, and the distribution frequently parallels the spine, with extension along the ribs. Diaphragmatic plaques are usually concentrated in the area of the central tendon (**Fig. 31**). Histologically, plaques are composed of coarse eosinophilic bundles of acellular collagen having a basket-weave pattern (**Fig. 32**). A variable degree of basophilic calcification is often present. Asbestos bodies are rarely identified histologically in plaques.

Diffuse pleural fibrosis, as opposed to pleural plaque, represents fibrous thickening of the parietal or visceral pleura often associated with dense pleural adhesions [McLoud et al. 1985]. The extent of fibrosis varies from minimal involvement to complete circumscription of the lung by a rind of thick fibrous tissue, resembling the gross appearance of malignant mesothelioma. Histologically, diffuse pleural fibrosis consists of coarse collagen bundles in a basket-weave pattern with focal calcification, resembling the histology of pleural plaques (**Fig. 33**) [Churg 1998b; Oury 2004; Roggli et al. 2010; Stephens et al. 1987]. An associated lesion occasionally seen in the lung beneath areas of diffuse pleural fibrosis or adherent pleural plaques is rounded atelectasis [Oury 2004; Hillerdal 1989; “Case records,” 1983] (**Fig. 34**). The pathogenesis of rounded atelectasis is thought to represent pleural infolding in conjunction with organizing pleuritis or pleural effusion (**Fig. 35**). Because of organization and fibrosis of the visceral pleural surface, the infolded pleura and surrounding atelectatic lung become irreversibly fixed in position. Macroscopically, the subpleural parenchyma is vaguely nodular, with a spongy texture surrounding a linear retraction of fibrotic visceral pleura. Histologically, compressed fibrotic alveolar parenchyma is oriented around a deep pleural fold, which can be highlighted with tissue elastic stains (**Fig. 35**). Although asbestos is considered to be the major cause, virtually any cause of pleural fibrosis can result in rounded atelectasis [Hilgenberg and Mark 1983].

Lung Cancer

Asbestos exposure increases the risk for lung carcinoma of all histological types [Churg 1998a]. The gross and microscopic appearance of lung carcinomas caused by asbestos is identical to that causally associated with tobacco smoke. An important variant of adenocarcinoma to recognize in the setting of asbestos exposure is pseudomesotheliomatous adenocarcinoma, in which a peripheral lung adenocarcinoma extensively infiltrates the pleura, causing pleural thickening that simulates diffuse pleural fibrosis or malignant mesothelioma [Harwood et al. 1976]. On pathological examination, the primary adenocarcinoma may be occult and difficult to identify. Other histological types of primary lung cancer or even metastatic tumors involving the pleura may generate a pseudomesotheliomatous appearance. In the series of pseudomesotheliomatous adenocarcinomas of Koss et al [1992], 17% had possible or definite asbestos exposure.

Pleural Mesothelioma

Asbestos exposure is the most important cause of pleural mesothelioma, a tumor that originates from the serosal surface [Hammar et al. 2008].The classical macroscopic appearance of malignant mesothelioma is that of a diffuse, thick rind of tumor encasing the lung, extending along the interlobar fissures, and infiltrating the chest wall, diaphragm, and mediastinal structures (**Fig. 36**). The pleural rind is usually thickest in the dependent regions of the thorax. Pleural mesotheliomas may exhibit nodularity or loculations filled with hemorrhagic fluid. The ipsilateral lung parenchyma is typically compressed by the expanding tumor burden.

Mesotheliomas are histologically diverse tumors with many different patterns and subtypes [Hammar et al. 2008]. The majority of mesotheliomas, however, fall into one of the categories of epithelioid, sarcomatoid, or biphasic subtypes, the latter having features of both sarcomatous and epithelial morphology. While mesotheliomas in general are regarded as nearly uniformly fatal, the sarcomatoid subtype carries an especially poor prognosis. Among sarcomatoid mesotheliomas, the desmoplastic variant often causes diagnostic challenges in the histological distinction from diffuse pleural fibrosis. In general, the histological separation of epithelioid mesothelioma from metastatic adenocarcinoma requires the use of a panel of immuno-histochemical stains, including relatively mesothelioma-specific markers like calretinin, cytokeratin 5/6, and WT-1, in addition to adenocarcinoma markers such as carcinoembryonic antigen, thyroid transcription factor 1, CD15, and B72.3. The distinction of sarcomatoid mesothelioma from primary or metastatic sarcomas of the pleura may be facilitated by immunostaining for keratin, which is usually positive in sarcomatoid mesotheliomas [Hammar et al. 2008].

Pathologic-Radiological Correlations

Silica and Coal Dust

Although the chest radiograph is an excellent method for assessing the degree of involvement of the lung in CWP and silicosis, certain limitations are recognized. Individual lesions less than 3 mm in maximal dimension may not be visualized radiographically [Vallyathan et al. 1996]. Therefore, in early macular CWP or nodular silicosis the chest radiograph may appear as “normal.” Radiologic summation effect due to the superimposition of numerous small nodules may nonetheless result in the appearance of small round opacities [Kleinerman et al. 1979]. The ILO system serves as a means of classifying chest radiographs of individuals with pneumoconiosis. It does not define pathologic entities. The distinction between CWP and silicosis by chest radiography alone is usually not possible. Nodular lesions of simple CWP and simple silicosis appear as rounded opacities measuring up to 1 cm in diameter on a chest radiograph [Cool et al. 2023; Kleinerman et al. 1979]. Small irregular opacities are less frequent. Lesions of PMF (complicated pneumoconiosis) are represented radiographically by large opacities that exceed 10 mm in the longest dimension.

Studies correlating lung pathology with ILO Classification in CWP have shown that small p-type opacities correlate with dust macules and emphysema (Fig. 20), (Fig. 21). Larger q- and r-type opacities are seen as fibrotic nodular lesions [Green and Vallyathan 1998; Ruckley et al. 1984a; Vallyathan et al. 1996]. Q-type opacities have been associated with nodular lesions measuring from 1 to 7 mm, while r-type opacities correlate with macronodules measuring from 7 to 10 mm [Vallyathan et al. 1996]. Ruckley et al [1984a] correlated stellate nodules (Fig. 17) with q-type opacities and round silicotic-type nodules with r-type opacities (Fig. 22). A positive correlation exists between mean weight of retained lung dust and radiographic profusion score for small round opacities in CWP [Ruckley et al. 1984a]. Small irregular opacities in coal workers are somewhat less frequent than rounded opacities and have been associated with emphysema or pigment-laden interstitial fibrosis (Fig. 27) [Lyons et al. 1974; Ruckley et al. 1984a].

In patients with rapidly progressive pneumoconiosis, features of silicosis were significantly associated with rounded (p, q, r) opacities on chest imaging, while high-grade interstitial fibrosis was associated with the presence of irregular (s, t, u) opacities [Cohen et al. 2016].

Asbestos-Related Pleuropulmonary Disease

In the ILO Classification, asbestosis is usually characterized by the development of small irregular opacities (s, t, u). In approximately 20% to 30% of cases, parenchymal changes are accompanied by pleural thickening with or without calcification. Rounded opacities are rarely seen in the chest radiographs of patients with asbestosis unless there has been additional exposure to silica. Progression of asbestosis may be seen radiographically as honeycomb change [Gefter et al. 1984; Morgan and Gee 1995].

Pleural changes due to asbestos exposure are identified more frequently on chest radiography than is parenchymal disease. Asbestos-related pleural effusion progressing to diffuse pleural thickening (fibrothorax) may create a ground-glass haze over the lung, associated with an obliterated costophrenic angle. With significant pleural fibrosis the rib spaces are crowded and there is ipsilateral loss of lung volume. Pleural plaques appear on the chest wall or diaphragm as smooth, regular linear shadows. En face plaques can closely mimic the parenchymal changes of asbestosis. Rounded atelectasis appears as a spherical or elliptical subpleural pleural-based opacity. Vessels and bronchi from the hilar region converge on the area of atelectasis, forming the “comet-tail” sign. Pleural thickening overlies the region of atelectasis, which can simulate a lung tumor [Gefter et al. 1984; Morgan and Gee 1995].

There are no distinctive radiologic features of lung carcinoma caused by asbestos exposure. There is a tendency, however, for increased lower-lobe distribution of asbestos-related lung cancers. Within the lower lobe, asbestos-related lung carcinomas are frequently peripherally distributed. In the presence of dense parenchymal fibrosis, radiographic detection of a neoplasm may be difficult [Gefter et al. 1984]. Attribution of a carcinoma to asbestos is supported by a significant cumulative exposure history or, from the pathological perspective, an elevated asbestos burden in the lung parenchyma, as assessed by asbestos bodies or fiber counts.

Finally, mesothelioma usually presents as a large unilateral pleural effusion. Pleural-based solid lesions may also occur in a minority of patients. With progression, tumor replaces pleural effusion, which often becomes loculated [Gefter et al. 1984; Morgan and Gee 1995].

References

Aberle DR, Gamsu G, Ray CS [1988a]. High-resolution CT of benign asbestos-related diseases: Clinical and radiographic correlation. Am J Roentgenol *151*(5):883–891, https://doi.org/10.2214/ajr.151.5.883.

Aberle DR, Gamsu G, Ray CS, Feuerstein IM [1988b]. Asbestos-related pleural and parenchymal fibrosis: Detection with high-resolution CT. Radiology *166*(3): 729–734, https://doi.org/10.1148/radiology.166.3.3340770.

Akira M, Higashihara T, Yokoyama K, Yamamoto S, Kita N, Morimoto S, Ikezoe J, Kozuka T [1989]. Radiographic type p pneumoconiosis: High-resolution CT. Radiology *171*(1):117–123, https://doi.org/10.1148/radiology.171.1.2928514.

Ameille J, Brochard P, Brechot JM, Pascano T, Cherin A, Raix A, Fredy M, Bignon J [1993]. Pleural thickening: A comparison of oblique chest radiographs and high-resolution computed tomography in subjects exposed to low levels of asbestos pollution. Int Arch Occup Environ Health *64*(8):545–548, https://doi.org/10.1007/BF00517698.

American Thoracic Society [2003]. American Thoracic Society Statement: occupational contribution to the burden of airway disease. Am J Respir Crit Care Med *167*(5):787–797, https://doi.org/10.1164/rccm.167.5.787.

American Thoracic Society [2004]. Diagnosis and initial management of nonmalignant diseases related to asbestos. Am J Resp Crit Care Med, *170*(6):691–715, https://doi.org/10.1164/rccm.200310-1436ST.

Antao VC, Petsonk EL, Sokolow LZ, Wolfe AL, Pinheiro GA, Hale JM, Attfield MD [2005]. Rapidly progressive coal workers' pneumoconiosis in the United States: geographic clustering and other factors. Occup Environ Med *62*(10):670–674, https://doi.org/10.1136/oem.2004.019679.

Bergin CJ, Muller NL, Vedal S, Chan-Yeung M [1986]. CT in silicosis: Correlation with plain films and pulmonary function tests. Am J Roentgenol *146*(3):477–483.

Blackley DJ, Halldin CN, Laney AS [2014]. Resurgence of a debilitating and entirely preventable respiratory disease among working coal miners. Am J Respir Crit Care Med *190*(6):708–709.

Blackley DJ, Laney AS, Halldin CN, Cohen RA [2015]. Profusion of opacities in simple coal worker's pneumoconiosis is associated with reduced lung function. Chest *148*(5):1293–1299, https://doi.org/10.1378/chest.15-0118.

Brichet A, Tonnel AB, Brambilla E, Devouassoux G, Rémy-Jardin M, Copin MC, Wallaert B [2002]. Chronic interstitial pneumonia with honeycombing in coal workers. Sarcoidosis Vasc Diffuse Lung Dis, *19*(3):211–219.

Brichet A, Wallaert B, Gosselin B, Remy-Jardin M, Voisin C, Lafitte JJ, Tonnel AB [1997]. ["Primary" diffuse interstitial fibrosis in coal miners: a new entity? study group on interstitial pathology of the society of thoracic pathology of the north]. In German. Rev Mal Respir *14*(4):277–285.

Buechner HA, Ansari A [1969]. Acute silico-proteinosis. a new pathologic variant of acute silicosis in sandblasters, characterized by histologic features resembling alveolar proteinosis. Dis Chest, *55*(4):274–284, https://doi.org/10.1378/chest.55.4.274.

Cahill BC, Harmon KR, Shumway SJ, Mickman JK, Hertz MI [1992]. Tracheobronchial obstruction due to silicosis. Am Rev Respir Dis, *145*(3):719–721, https://doi.org/10.1164/ajrccm/145.3.719.

Case records of the Massachusetts General Hospital [1983]. Weekly clinicopathological exercises. Case 24-1983. A 61-year-old man with a peripheral lung mass. N Engl J Med, 308(24):1466-1472.

CDC [2007]. Fixed obstructive lung disease among workers in the flavor-manufacturing industry—California, 2004–2007. MMWR *56*(16), 389–393.

Churg A [1998a]. Neoplastic asbestos-induced disease. In: Churg A, Green FHY, eds. Pathology of Occupational Lung Disease 2nd ed. Baltimore, MD: Williams & Wilkins, 339–392.

Churg A [1998b]. Nonneoplastic disease caused by asbestos. In: Churg A, Green FHY, eds. Pathology of Occupational Lung Disease 2nd ed. Baltimore, MD: Williams & Wilkins, 277–338.

Cockcroft A, Seal RM, Wagner JC, Lyons JP, Ryder R, Andersson N [1982]. Post-mortem study of emphysema in coalworkers and non-coalworkers. Lancet, *2*(8298):600–603.

Cockcroft A, Lyons JP, Andersson N, Saunders MJ [1983]. Prevalence and relation to underground exposure of radiological irregular opacities in South Wales coal workers with pneumoconiosis. Br J Ind Med *40*(2):169–172.

Cohen RA, Petsonk EL, Rose C, Young B, Regier M, Najmuddin A, Abraham JL, Churg A, Green FH [2016]. Lung pathology in U.S. coal workers with rapidly progressive pneumoconiosis implicates silica and silicates. Am J Respir Crit Care Med *193*(6):673–680, https://doi.org/10.1164/rccm.201505-1014OC.

Collins HP, Dick JA, Bennett JG, Pern PO, Rickards MA, Thomas DJ, Washington JS, Jacobsen M [1988]. Irregularly shaped small shadows on chest radiographs, dust exposure, and lung function in coalworkers' pneumoconiosis. Br J Ind Med *45*(1):43-55, https://doi.org/10.1136/oem.45.1.43.

Cool CD, Murray J, Vorajee NI, Rose CS, Zell-Baran, LM, Sanyal S, Franko AD, Almberg KS, Iwaniuk C, Go L, Green F , Cohen RA [2023]. Pathologic findings in severe coal workers' pneumoconiosis in contemporary US coal miners. Arch Pathol Lab Med *148*(7):805–817, https://doi.org/10.5858/arpa.2022-0491-OA.

Cox CW, Lynch DA [2015]. Medical imaging in occupational and environmental lung disease. Curr Opin Pulm Med *21*(2):163–170, https://doi.org/10.1097/MCP.0000000000000139.

Craighead J, Kleinerman J, Abraham JL, Gibbs AR, Green FHY, Harley RA, Ruettner JR, Vallyathan V, Juliano EB. [1988]. Diseases associated with exposure to silica and nonfibrous silicate minerals. Arch Pathol Lab Med *112*(7):673–720, https://www.ncbi.nlm.nih.gov/pubmed/2838005.

Cullinan P, McGavin CR, Kreiss K, Nicholson AG, Maher TM, Howell T, Banks J, Newman Taylor AJ, Chen CH, Tsai PJ, Shih TS, Burge PS [2013]. Obliterative bronchiolitis in fibreglass workers: a new occupational disease? Occup Environ Med *70*(5):357–359, https://doi.org/10.1136/oemed-2012-101060.

Dick JA, Morgan WK, Muir DF, Reger RB, Sargent N [1992]. The significance of irregular opacities on the chest roentgenogram. Chest, *102*(1):251–260, https://doi.org/10.1378/chest.102.1.251.

Eisner MD, Anthonisen N, Coultas D, Kuenzli N, Perez-Padilla R, Postma D, Romieu I, Silverman EK, Balmes JR [2010]. An official American Thoracic Society public policy statement: novel risk factors and the global burden of chronic obstructive pulmonary disease. Am J Respir Crit Care Med *182*(5):693–718, https://doi.org/10.1164/rccm.200811-1757ST.

Erkinjuntti-Pekkanen R, Rytkonen H, Kokkarinen JI, Tukiainen HO, Partanen K, Terho EO [1998]. Long-term risk of emphysema in patients with farmer's lung and matched control farmers. Am J Respir Crit Care Med *158*(2):662–665, https://doi.org/10.1164/ajrccm.158.2.9710012.

Gaensler EA, Kaplan AI [1971]. Asbestos pleural effusion. Ann Intern Med, *74*(2):178–191, https://doi.org/10.7326/0003-4819-74-2-178.

Gefter WB, Epstein DM, Miller WT [1984]. Radiographic evaluation of asbestos-related chest disorders. Crit Rev Diagn Imaging, *21*(2):133–181.

Gevenois PA, de Maertelaer V, Madani A, Winant C, Sergent G, De Vuyst P [1998]. Asbestosis, pleural plaques and diffuse pleural thickening: Three distinct benign responses to asbestos exposure. Eur Respir J *11*(5):1021–1027, https://doi.org/10.1183/09031936.98.11051021.

Gibbs AR, Wagner JC [1998]. Diseases due to silica. In: Churg A, Green FHY, eds. Pathology of Occupational Lung Disease. 2nd ed. Baltimore, MD: Williams & Wilkins, 209–234.

Gottschall EB [2002]. Occupational and environmental thoracic malignancies. J Thorac Imaging *17*(3):189–197, https://doi.org/10.1097/00005382-200207000-00003.

Gough J, Rivers D, Seal RM [1955]. Pathological studies of modified pneumoconiosis in coal-miners with rheumatoid arthritis; Caplan's syndrome. Thorax, *10*(1):9–18, https://doi.org/10.1136/thx.10.1.9.

Green F, Brower P, Vallyathan V, Attfield M [1998]. Coal mine dust exposure and type of pulmonary emphysema in coal workers. In: Chiyotani D, Hosoda Y, Aizawa Y, eds. Advances in the prevention of occupational respiratory diseases. Amsterdam: Elsevier Science BV.

Green FHY, Vallyathan V [1998]. Coal workers' pneumoconiosis and pneumoconiosis due to other carbonaceous dusts. In: Churg A, Green FHY, eds. Pathology of Occupational Lung Disease. 2nd ed. Baltimore, MD: Williams & Wilkins, 129–208.

Halldin CN, Blackley DJ, Markle T, Cohen RA, Laney AS [2020]. Patterns of progressive massive fibrosis on modern coal miner chest radiographs. Archives of Environmental & Occupational Health *75*(3):152–158, https://doi.org/10.1080/19338244.2019.1593099.

Hammar SP, Henderson DW, Klebe S, Dodson RF [2008]. Neoplasms of the pleura. In: Tomashefski JF Jr, Cagle PT, Farver CF, Fraire AE, eds. Dail and Hammar's Pulmonary Pathology Volume II. 3rd ed. New York, NY: Springer, 558–734, https://doi.org/10.1007/978-0-387-68792-6.

Harber P, Tashkin DP, Simmons M, Crawford L, Hnizdo E, Connett J, Lung Health Study G [2007]. Effect of occupational exposures on decline of lung function in early chronic obstructive pulmonary disease. Am J Respir Crit Care Med *176*(10):994–1000, https://doi.org/10.1164/rccm.200605-730OC.

Harkin TJ, McGuinness G, Goldring R, Cohen H, Parker JE, Crane M, Naidich DP, Rom WN [1996]. Differentiation of the ILO boundary chest roentgenograph (0/1 to 1/0) in asbestosis by high-resolution computed tomography scan, alveolitis, and respiratory impairment. J Occup Environ Med *38*(1):46–52, https://doi.org/10.1097/00043764-199601000-00016.

Harwood TR, Gracey DR, Yokoo H [1976]. Pseudomesotheliomatous carcinoma of the lung. a variant of peripheral lung cancer. Am J Clin Pathol, *65*(2):159–167, https://doi.org/10.1093/ajcp/65.2.159.

Hering KG [1992]. [Evaluation and classification of CT findings in work-related lung and pleural changes in accordance with the ILO pneumoconiosis classification]. In German. Rontgenpraxis *45*(9):304–308.

Hering KG, Tuengerthal S, Kraus T [2004]. [Standardized CT/HRCT-classification of the German federal republic for work and environmental related thoracic diseases]. In German. Der Radiologe *44*(5):500–511, https://doi.org/10.1007/s00117-004-1027-7.

HHS [2012]. Specifications for medical examinations of underground coal miners. Final Rule. Fed Regist *77*(178): 56718, https://www.federalregister.gov/documents/2012/09/13/2012-22253/specifications-for-medical-examinations-of-underground-coal-miners.

Hilgenberg AD, Mark EJ [1983]. Case 24-1983. A 61-year-old man with a peripheral lung mass. N Engl J Med, *308*(24):1466–1472, https://doi.org/10.1056/NEJM198306163082408.

Hillerdal G [1989]. Rounded atelectasis. Clinical experience with 74 patients. Chest, 95(4):836-841.

Hnizdo E, Murray J, Davison A [2000]. Correlation between autopsy findings for chronic obstructive airways disease and in-life disability in South African gold miners. Int Arch Occup Environ Health *73*(4):235–244, https://doi.org/10.1007/s004200050423.

Hnizdo E, Sluis-Cremer GK, Abramowitz JA [1991]. Emphysema type in relation to silica dust exposure in South African gold miners. Am Rev Respir Dis *143*(6):1241–1247, https://doi.org/10.1164/ajrccm/143.6.1241.

Hodgson MJ, Parkinson DK, Karpf M [1989]. Chest x-rays in hypersensitivity pneumonitis: a metaanalysis of secular trend. Am J Ind Med *16*(1),45–53, https://doi.org/10.1002/ajim.4700160106.

Honma K, Chiyotani K [1993]. Diffuse interstitial fibrosis in nonasbestos pneumoconiosis–a pathological study. Respiration *60*(2):120–126.

Huuskonen O, Kivisaari L, Zitting A, Taskinen K, Tossavainen A, Vehmas T [2001]. High-resolution computed tomography classification of lung fibrosis for patients with asbestos-related disease. Scand J Work Environ Health *27*(2):106–112.

International Labour Office (ILO) [2023]. Guidelines for the use of the ILO International Classification of Radiographs of Pneumoconioses—revised edition 2022. Geneva, Switzerland: International Labour Organization, http://www.ilo.org/global/topics/safety-and-health-at-work/resources-library/publications/WCMS_867859/lang--en/index.htm.

Katabami M, Dosaka-Akita H, Honma K, Saitoh Y, Kimura K, Uchida Y, Mikami H, Ohsaki Y, Kawakami Y, Kikuchi K [2000]. Pneumoconiosis-related lung cancers: Preferential occurrence from diffuse interstitial fibrosis-type pneumoconiosis. Am J Respir Crit Care Med *162*(1):295–300, https://doi.org/10.1164/ajrccm.162.1.9906138.

King MS, Eisenberg R, Newman JH, Tolle JJ, Harrell FE, Jr., Nian H, Ninan M, Lambright ES, Sheller JR, Johnson JE, Miller RF [2011]. Constrictive bronchiolitis in soldiers returning from Iraq and Afghanistan. N Engl J Med *365*(3):222–230, https://doi.org/10.1056/NEJMoa1101388.

Kinsella M, Muller N, Vedal S, Staples C, Abboud RT, Chan-Yeung M [1990]. Emphysema in silicosis. a comparison of smokers with nonsmokers using pulmonary function testing and computed tomography. Am Rev Respir Dis *141*(6):1497–1500, https://doi.org/10.1164/ajrccm/141.6.1497.

Kleinerman J, Green F, Harley RA, Lapp L, Laqueur W, Naeye RL, Pratt P, Taylor G, Wiot J, Wyatt J [1979]. Pathology standards for coal workers' pneumoconiosis. Arch Pathol Lab Med, *103*(8), 375–432.

Koss M, Travis W, Moran C, Hochholzer L [1992]. Pseudomesotheliomatous adenocarcinoma: a reappraisal. Semin Diagn Pathol, *9*(2):117–123.

Kraus T, Borsch-Galetke E, Elliehausen HJ, Frank K, Hering KG, Hieckel HG, Hofmann-Preiss K, Jacques W, Jeremie U, Kotschy-Lang N, Mannes E, Otten H, Raab W, Raithel HJ, Schneider WD, Tuengerthal S [2009]. [Recommendations for reporting benign asbestos-related findings in chest x-ray and CT to the accident insurances]. In German. Pneumologie *63*(12):726–732, https://doi.org/10.1055/s-0029-1215322.

Kreuzer M, Sogl M, Bruske I, Mohner M, Nowak D, Schnelzer M, Walsh L [2013]. Silica dust, radon and death from non-malignant respiratory diseases in German uranium miners. Occup Environ Med *70*(12):869–875, https://doi.org/10.1136/oemed-2013-101582.

Kuempel ED, Wheeler MW, Smith RJ, Vallyathan V, Green FH [2009]. Contributions of dust exposure and cigarette smoking to emphysema severity in coal miners in the United States. Am J Respir Crit Care Med *180*(3):257–264, https://doi.org/10.1164/rccm.200806-840OC.

Kusaka Y, Hering KG, Parker JE [2005]. International classification of HRCT for occupational and environmental respiratory diseases. Tokyo, Japan: Springer.

Laney AS, Petsonk EL [2012]. Small pneumoconiotic opacities on U.S. coal worker surveillance chest radiographs are not predominantly in the upper lung zones. Am J Ind Med *55*(9):793–798, https://doi.org/10.1002/ajim.22049.

Leigh J [1990]. Fifteen-year longitudinal studies of FEV1 loss and mucus hypersecretion development in coal workers in New South Wales, Australia. In: Proceedings of the VIIth International Pneumoconioses Conference Part II. US Department of Health and Human Services, Centers for Disease Control, National Institute for Occupational Safety and Health, DHHS (NIOSH). Publication No. 90-108, http://www.cdc.gov/niosh/docs/90-108/.

Lynch DA, Gamsu G, Ray CS, Aberle DR [1988]. Asbestos-related focal lung masses: manifestations on conventional and high-resolution CT scans. Radiology *169*(3):603–607, https://doi.org/10.1148/radiology.169.3.3186982.

Lynch DA, Rose CS, Way D, King TE Jr. [1992]. Hypersensitivity pneumonitis: sensitivity of high-resolution CT in a population-based study. Am J Roentgenol *159*(3):469–472, https://doi.org/10.2214/ajr.159.3.1503007.

Lyons JP, Ryder RC, Campbell H, Clarke WG, Gough J [1974]. Significance of irregular opacities in the radiology of coalworkers' pneumoconiosis. Br J Ind Med, *31*(1):36–44.

Mayo JR [2009]. CT evaluation of diffuse infiltrative lung disease: dose considerations and optimal technique. J Thorac Imaging *24*(4):252–259, https://doi.org/10.1097/RTI.0b013e3181c227b2.

McConnochie K, Green FHY, Vallyathan V, Wagner JC, Seal RME, Lyons JP [1988]. Interstitial fibrosis in coal workers—experience in Wales and West Virginia. Ann Occup Hyg 32:553-560, https://doi.org/10.1093/annhyg/32.inhaled_particles_VI.553.

McHugh K, Blaquiere, RM [1989]. CT features of rounded atelectasis. Am J Roentgenol *153*(2) 257–260, https://doi.org/10.2214/ajr.153.2.257.

McCloud TC, Woods BO, Carrington CB, Epler GR, Gaensler EA [1985]. Diffuse pleural thickening in an asbestos-exposed population: prevalence and causes. AJR Am J Roentgenol *144*(1):9–18, https://doi.org/10.2214/ajr.144.1.9.

Morgan WKC, Gee JBL [1995]. Asbestos-related diseases. In: Morgan WKC, Seaton A, eds. Occupational Lung Diseases. 3rd ed. Philadelphia, PA: WB Saunders, 308–373.

Naccache JM, Marchand-Adam S, Kambouchner M, Guillon F, Monnet I, Girard F, Brauner M, Valeyre D [2003]. Ground-glass computed tomography pattern in chronic beryllium disease: pathologic substratum and evolution. J Comput Assist Tomogr *27*(4):496–500, https://doi.org/10.1097/00004728-200307000-00007.

Newman LS, Buschman DL, Newell JD, Jr., Lynch DA [1994]. Beryllium disease: Assessment with CT. Radiology *190*(3):835–840, https://doi.org/10.1148/radiology.190.3.8115636.

NIOSH [2011]. Coal mine dust exposures and associated health outcomes-a review of information published since 1995. Cincinnati, OH: U.S. Department of Health and Human Services, Centers for Disease Control and Prevention, National Institute for Occupational Safety and Health, DHHS (NIOSH) Publication No. 2011-172, https://www.cdc.gov/niosh/docs/2011-172/.

Oury TD [2004]. Benign asbestos-related pleural disease. In: Roggli VL, Oury TD, Sporn TA, eds. Pathology of Asbestos-Associated Diseases, 2nd ed. New York, NY: Springer, 169–192.

Petsonk EL, Rose C, Cohen R [2013]. Coal mine dust lung disease. New lessons from old exposure. Am J Respir Crit Care Med *187*(11):1178–1185, https://doi.org/10.1164/rccm.201301-0042CI.

Remy-Jardin M, Degreef JM, Beuscart R, Voisin C, Remy J [1990]. Coal worker's pneumoconiosis: CT assessment in exposed workers and correlation with radiographic findings. Radiology *177*(2):363–371, https://doi.org/10.1148/radiology.177.2.2217770.

Rogan JM, Attfield MD, Jacobsen M, Rae S, Walker DD, Walton WH [1973]. Role of dust in the working environment in development of chronic bronchitis in British coal miners. Br J Ind Med *30*(3): 217–226.

Roggli VL [2004]. Asbestos bodies and nonasbestos ferruginous bodies. In: Roggli VL, Oury TD, Sporn TA, eds. Pathology of Asbestos-Associated Diseases. 2nd ed. New York, NY: Springer, 34–70.

Roggli VL, Sharma A [2004]. Analysis of tissue mineral fiber content. In: Roggli VL, Oury TD, Sporn TA, eds. Pathology of Asbestos-Associated Diseases 2nd ed. New York, NY: Springer, 309–354.

Roggli VL, Gibbs AR, Attanoos R, et al. [2010]. Pathology of asbestosis—an update of the diagnostic criteria. report of the Asbestosis Committee of the College of American Pathologists and Pulmonary Pathology Society. Arch Pathol Lab Med, *134*(3):462–480, https://doi.org/10.5858/134.3.462.

Ruckley VA, Fernie JM, Chapman JS, et al. [1984a]. Comparison of radiographic appearances with associated pathology and lung dust content in a group of coalworkers. Br J Ind Med *41*(4):459–467.

Ruckley VA, Gauld SJ, Chapman JS, Davis JM, Douglas AN, Fernie JM, Jacobsen M, Lamb D [1984b]. Emphysema and dust exposure in a group of coal workers. Am Rev Respir Dis *129*(4):528-532, https://www.ncbi.nlm.nih.gov/pubmed/6711995.

Sargent EN, Boswell WD, Jr., Ralls PW, Markovitz A [1984]. Subpleural fat pads in patients exposed to asbestos: distinction from non-calcified pleural plaques. Radiology *152*(2):273–277, https://doi.org/10.1148/radiology.152.2.6739783.

Silva CI, Muller NL, Lynch DA, Curran-Everett D, Brown KK, Lee KS, Chung MP, Churg A [2008]. Chronic hypersensitivity pneumonitis: Differentiation from idiopathic pulmonary fibrosis and nonspecific interstitial pneumonia by using thin-section CT. Radiology *246*(1):288–297, https://doi.org/10.1148/radiol.2453061881.

Staples CA, Gamsu G, Ray CS, Webb WR [1989]. High resolution computed tomography and lung function in asbestos-exposed workers with normal chest radiographs. Am Rev Respir Dis, *139*(6):1502–1508, https://doi.org/10.1164/ajrccm/139.6.1502.

Stephens M, Gibbs AR, Pooley FD, Wagner JC [1987]. Asbestos induced diffuse pleural fibrosis: pathology and mineralogy. Thorax *42*(8):583–588, https://doi.org/10.1136/thx.42.8.583.

Suganuma N, Kusaka Y, Hering KG, Vehmas T, Kraus T, Parker JE, Shida H [2006]. Selection of reference films based on reliability assessment of a classification of high-resolution computed

tomography for pneumoconioses. Int Arch Occup Environ Health *79*(6):472–476, https://doi.org/10.1007/s00420-005-0067-2.

Tamura T, Suganuma N, Hering KG, Vehmas T, Itoh H, Akira M, Takashima Y, Hirano H, Kusaka Y [2015]. Relationships (I) of international classification of high-resolution computed tomography for occupational and environmental respiratory diseases with the ILO international classification of radiographs of pneumoconioses for parenchymal abnormalities. Ind Health *53*(3):260–270, https://doi.org/10.2486/indhealth.2014-0073.

The National Lung Screening Trial Research Team. [2011]. Reduced lung-cancer mortality with low-dose computed tomographic screening. N Engl J Med *365*(5):395–409, https://doi.org/10.1056/NEJMoa1102873.

US Preventive Services Task Force [2021]. Screening for lung cancer: US Preventive Services Task Force recommendation statement. JAMA *325*(10):962, https://doi.org/10.1001/jama.2021.1117.

Vallyathan V, Brower PS, Green FH, Attfield MD [1996]. Radiographic and pathologic correlation of coal workers' pneumoconiosis. Am J Respir Crit Care Med *154*(3):741–748.

Young RC, Jr., Rachal RE, Carr PG, Press HC [1992]. Patterns of coal workers' pneumoconiosis in Appalachian former coal miners. J Natl Med Assoc *84*(1):41–48.

SUBSET 1 – Radiograph Classification

Introduction

For eight decades, the ILO has published guidelines on how to classify radiographs of patients with pneumoconiosis. This section reviews the *Guidelines for the Use of the ILO International Classification of Radiographs of the Pneumoconioses* [ILO 2023]. The discussion follows the sequence of items found on the NIOSH classification form for reporting findings potentially associated with pneumoconiosis in chest radiographs of workers exposed to hazardous dust (Chest Radiograph Classification Form).

The classification form allows for systematic recording of radiographic findings for all pneumoconiosis types. It is designed only for reporting the findings on a posteroanterior view of the chest, even though other views are used in the clinical assessment of a patient. The information recorded using the classification form may contribute to the evaluation of a worker for compensation but the ILO classification system itself is not intended to set or imply a level at which compensation may be payable.

The complete classification is discussed in this subset, although an abbreviated classification as described in the ILO Guidelines may be used in whole or in part in some circumstances. For the abbreviated classification, less detailed recording is performed (e.g., pleural thickening is noted only with the symbol **"PT"**). The uncommon occurrence of pleural changes in CWP may in some settings allow use of the short classification for recording these findings, whereas use of the complete classification is more appropriate for recording the parenchymal small opacities found in this entity. A statement should be made in the **"Comments"** section of the form if the abbreviated classification is used.

No radiographic features are pathognomonic of dust exposure. Some radiographic findings seen with pneumoconiosis may also be present with other disease processes. Even if conditions other than pneumoconiosis are included within the radiologic differential diagnosis, the posteroanterior view should be classified if:

1. Any pleural or parenchymal findings consistent with a pneumoconiosis are present, and
2. Pneumoconiosis is included within the radiologic differential diagnosis.

Some appearances are consistent with pneumoconiosis, while others are not. Those that are consistent or potentially consistent should be classified and recorded. Those that clearly are not consistent should be indicated in the **"Symbols"** and **"Comments"** sections of the form.

If pneumoconiosis is thought to be a possible cause of appearances on the chest radiograph, then those appearances should be classified and recorded. Thus, if the findings might be secondary to pneumoconiosis but other etiologies are also to be considered, the classification for pneumoconiosis (Sections 2A through 3D) should be completed and the other potential etiologies also noted under **4A** to **4E** in the **"Symbols"** and **"Comments"** sections.

If pneumoconiosis is not at all in the differential diagnosis and all appearances are thought to be secondary to a process other than pneumoconiosis, then this should be indicated in Sections **2A** and **3A**, and the findings and opinion should be recorded under Sections **4A** to **4E** in the **"Symbols"** and **"Comments"** sections.

Radiograph Identification

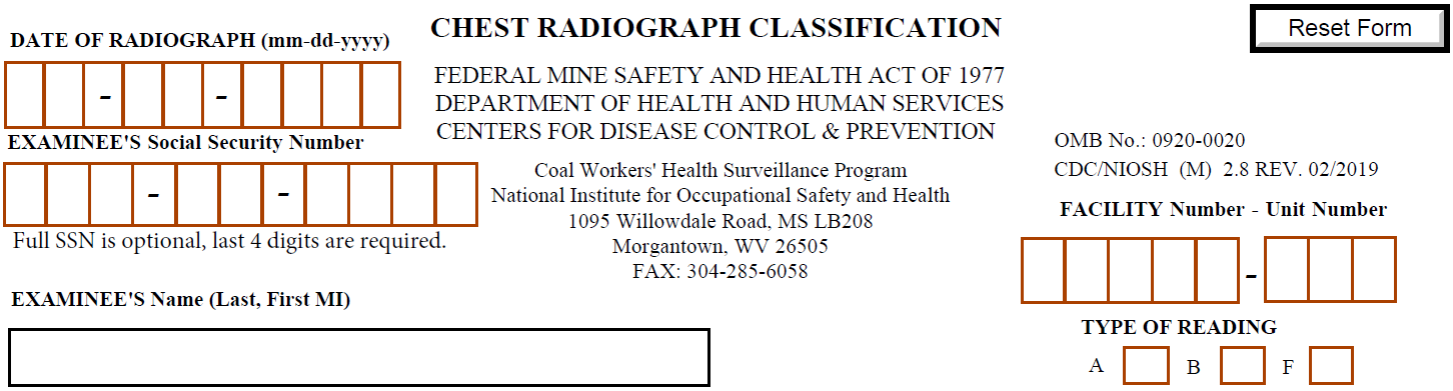
DATE OF RADIOGRAPH (mm-dd-yyyy)

EXAMINEE'S Social Security Number

Full SSN is optional, last 4 digits are required.

EXAMINEE'S Name (Last, First MI)

CHEST RADIOGRAPH CLASSIFICATION

FEDERAL MINE SAFETY AND HEALTH ACT OF 1977
DEPARTMENT OF HEALTH AND HUMAN SERVICES
CENTERS FOR DISEASE CONTROL & PREVENTION

Coal Workers' Health Surveillance Program
National Institute for Occupational Safety and Health
1095 Willowdale Road, MS LB208
Morgantown, WV 26505
FAX: 304-285-6058

Reset Form

OMB No.: 0920-0020
CDC/NIOSH (M) 2.8 REV. 02/2019

FACILITY Number - Unit Number

TYPE OF READING
A B F

Note: Please record your interpretation of a single radiograph by placing an "x" in the appropriate boxes on this form. Classify all appearances described in the ILO International Classification of Radiographs of Pneumoconiosis or Illustrated by the ILO Standard Radiographs. Use symbols and record comments as appropriate.

Date of Radiograph

Enter the month, day, year of the radiograph or study date.

Social Security Number

Entering the examinee's full Social Security Number is optional. The last four digits of the Social Security Number are required if available and not already recorded.

Name

Enter the examinee's full name. Last, First, and Middle Initial.

Type of Reading

These blocks refer to the qualification of the reader or readers. "A" indicates the reading has been made by an "A Reader"; "B" by a "B Reader"; and "F" for facility or clinical reading. See the appended reprint from the Federal Register for definitions of "A" and "B" readers.

Note: F ("Facility") reading is by a physician who has been determined to be qualified to interpret chest radiographs by a licensed clinical health care facility.

Check the box "A", "B", or "F" appropriate to your qualifications.

Facility Number

This number identifies the NIOSH certified facility and radiograph unit conducting the radiographic examination.

Section 1: Image Quality

Assessment of image technical quality is critically important before performing an ILO classification. Therefore, quality appraisals are the first items recorded on the classification form. Historically, variations in image quality have had an important effect on the small opacity profusion category selected by the reader. The quality of modern digital chest radiographs is often better than hard copy images, especially with appropriate use of window and level functions. However, regardless of the imaging modality, readers completing ILO classifications should assess the quality of the image in each lung zone. Depending on the type of opacities being evaluated, the appearance and perception may be altered, accentuated, or diminished. Quality effects may be generalized throughout the image or limited to specific lung zones.

Factors that can influence perception of opacities may include image contrast, resolution, exposure, or gray scale, as well degree of inflation, body position, or movement during the examination. Localized effects may be due to superimposed bony structures, soft tissues, or foreign bodies (e.g., pacemakers, tubing, clothing). Digital radiographic systems should be monitored to avoid linear artifacts, or noise/mottle, and excessive edge enhancement, which can suggest p-type pneumoconiotic opacities. Image noise or mottle, caused by inadequate exposure, is commonly encountered in systems geared to reduce radiation dose. Inadequate exposure cannot be fixed with modern digital systems by alterations in window and leveling or post processing. Post processing software functions should be set to the minimum edge enhancement permitted by the system to facilitate comparisons to ILO digital standard radiographs.

After selecting one or two standard images that visually appear to match the subject radiograph most closely, the reader should weigh the potential impact of any quality factors on the appearance of parenchymal opacities. When deemed necessary, an adjustment of the profusion category may be appropriate, based upon the anticipated influence of quality factors on the comparison of the subject radiograph and the ILO standard. If more than a minor adjustment is judged necessary, consideration should be given, whenever possible, to obtaining a better quality radiograph, and classifying the imperfect image as unreadable.

There are four grades of radiographic quality:

1. Good, free of technical imperfections or artifacts.
2. Acceptable, with no technical defects or artifacts likely to impair classification of the radiograph for pneumoconiosis.
3. Acceptable, with technical defects or artifacts but still adequate for classification purposes.
4. “U/R”, unreadable or unacceptable for classification purposes.

Minor errors in positioning and handling artifacts that do not overlie the heart or lungs would usually be classified “2”. Minor degrees of overexposure or underexposure, and minor departures from proper radiographic contrast that do not preclude the classification of the radiograph, should be classified as “3”. Images with gross overexposure or underexposure, gross unsharpness, and gross departures from proper radiographic contrast should all be classified “U/R”. The Federal Register Part 718 Appendix A details the standards for the administration and interpretation of x-rays for the Black Lung Program. If the technical quality is not grade “1”, an indication of the technical defect must be made.

Check the box with “1,” “2,” “3,” or “U/R” that best indicates the quality of the radiograph.
You may wish to wait until you have attempted to classify the radiograph before deciding whether its “quality” may affect your interpretation.
If you check box “2,” “3,” or “U/R”, indicate the reason(s) by marking all boxes that apply, and specify “other defects” on the adjacent lines.

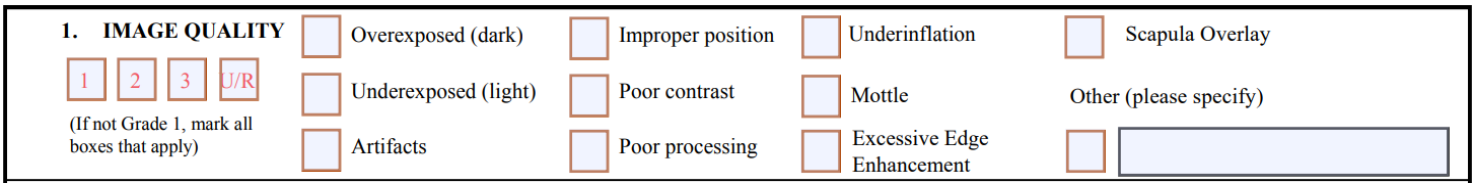

Text Captions

Section 2: Parenchymal Abnormalities

2A. Any Classifiable Parenchymal Abnormalities?

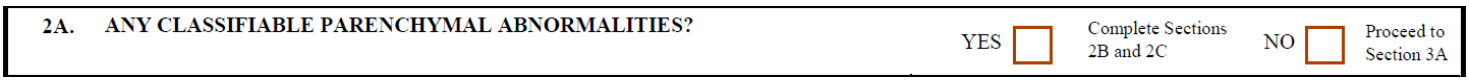

You must check “YES” or “NO”.
If “YES”, complete Sections 2B and 2C.
If “NO”, proceed to Section 3A.

2B. Small Opacities

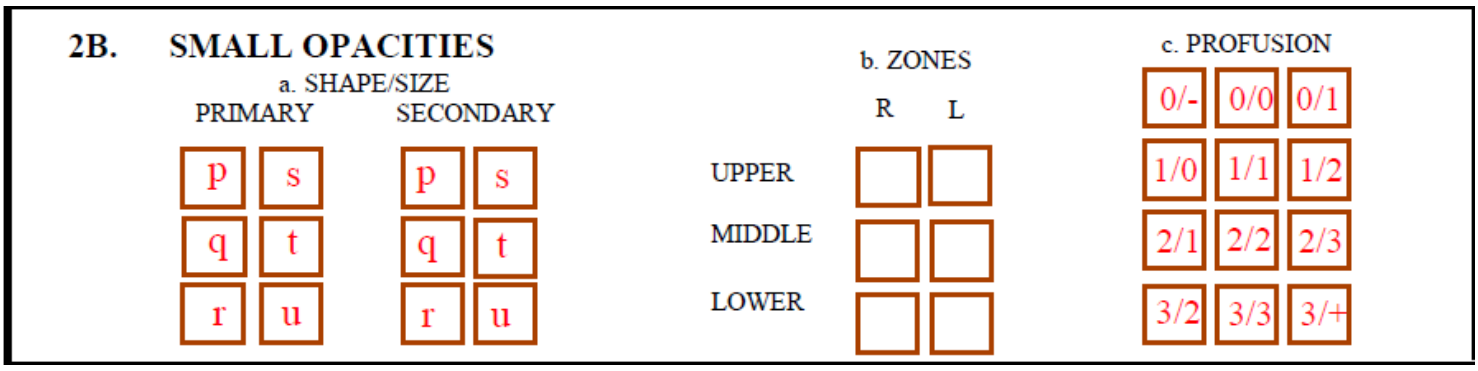

a. Shape/Size (Radiographs #1 to #3)

The various sizes and shapes of small opacities are represented by the letters "p", "q", "r", "s", "t", and "u". The small opacities' shape may be rounded ("p", "q", "r") or irregular ("s", "t", "u"). In previous classification schemes, irregular opacities have been described as "blotchy", "reticular", "linear", network", and "fibrotic". The small opacities associated with asbestos exposure are usually irregular or linear. Those associated with exposure to silica are usually rounded. Mixed-dust exposures such as coal mining may produce either or both.

Radiograph #1

Demonstrates the difference in appearance between small rounded and small irregular opacities.

Radiograph 1p demonstrates excellent examples of p opacities between the left 2nd and 3rd anterior interspaces. Radiographs 1q and 1r show good examples of those opacity types respectively.

Radiograph 1s shows good examples of s opacities.
Radiograph 1t the right lower zone shows good examples of t opacities.
Radiograph 1u is the ILO analog standard for u opacities. Chest radiographs with u opacities are very rarely seen.

With respect to size, small, rounded opacities are defined in terms of their diameters.

p = Up to about 1.5 mm
q = Diameters exceed 1.5 mm and up to about 3 mm
r = Diameters exceed 3 mm and up to about 10 mm

The sizes of small irregular opacities are expressed in terms of their widths:

s = Up to about 1.5 mm
t = Widths exceed 1.5 mm and up to about 3 mm
u = Widths exceed 3 mm and up to about 10 mm

Radiograph #2

Presents a normal study, but then illustrates the differences in diameter that characterize small rounded (**p**, **q**, **r**) opacities.

Radiograph #3

Illustrates the differences in width that characterize small irregular (**s**, **t**, **u**) opacities.

Because u opacities are rare, radiograph 3u uses the current analog ILO standard as an example.

Note that the classification form has two sections for recording the size and shape of small opacities: primary and secondary. Determine the size and shape of any small opacities that may be present by comparing the subject radiograph with ILO Digital Standard Radiographs, which take precedence over written definitions. In the **primary** block, check the letter that refers to the size and shape of small opacities that predominate. If small opacities of some other size and shape are also present in significant numbers, check the letter that refers to the next most numerous opacity type in the **secondary** block. If virtually all small opacities are of the same size and shape, check the same letter in both the **primary** and **secondary** blocks.

Note: It is customary when referring to the primary and secondary types of opacities in a radiograph to separate the primary and secondary notations by a forward slash (/) with the primary type of opacity occurring before the slash and the secondary type after the slash. For example, among the 2022 Standard ILO Film Radiographs, one was identified as 3/3 **t/s** (the primary type of opacity is t; the secondary type is s) or 2/2 **t/t** (nearly all opacities are t-type). Note that in any single radiograph there may be only rounded opacities (**p**, **q**, **r**), only irregular opacities (**s**, **t**, **u**), or both rounded and irregular.

b. Zones

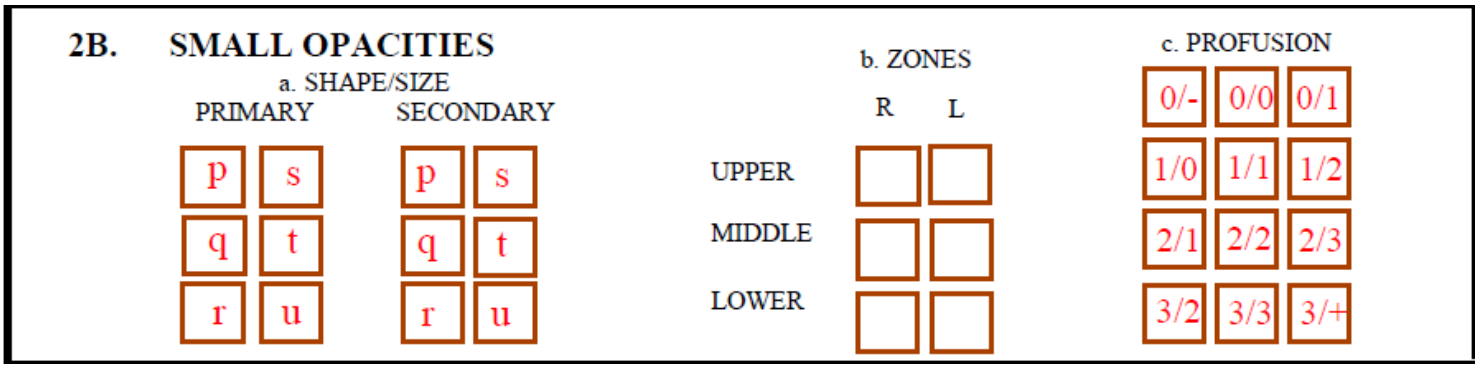

Once the size and shape of the small opacities have been determined, the areas of involvement are indicated. For this purpose, the lungs are divided into an upper, middle, and lower zone on each side by imaginary horizontal lines traversing the lungs at levels one-third and two-thirds of the vertical distance between the apices and the hemidiaphragmatic domes. On the report form, zones of involvement are represented by six boxes arranged in two vertical columns representing the right and left lungs.

Within each vertical column, the boxes from top to bottom represent the upper, middle, and lower zones, respectively.

Check each box in the **Zones** block that represents a zone where small opacities are thought to be present.

c. Profusion (Radiographs #4 to #10)

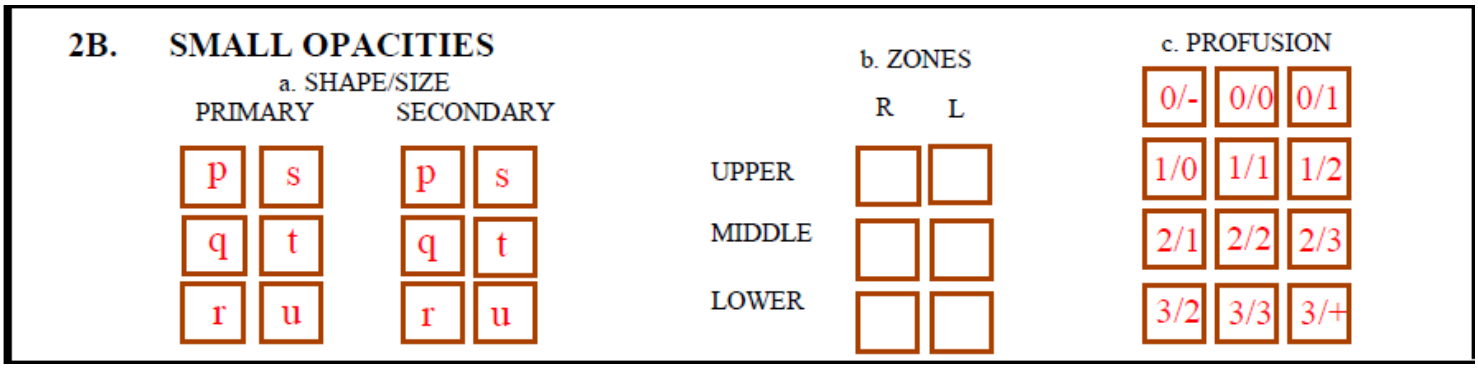

After defining the character (size and shape) of any pneumoconiotic small opacities that may be present and indicating their distribution in terms of lung zones, it is necessary to determine their profusion (concentration, number per unit area). Profusion is expressed in terms of four major categories: **0**, **1**, **2** and **3**. These span the range from no small opacities present (**0**) to a maximal number present (**3**). Successively higher numbers represent progressively greater numbers of small opacities per unit area.

The profusion of small opacities is determined by visual comparison of the subject radiograph with ILO Standards representing the mid ranges of the four major categories. Profusion is a continuum, and clinical radiographs often do not match any one ILO Standard. Rather, they may appear to fall somewhere between two standards. In recognition of this, each major category is divided into three "minor" categories, creating a 12 point scale.

Major Categories: 0 1 2 3
Minor Categories: 0/-,0/0,0/1; 1/0,1/1,1/2; 2/1,2/2,2/3; 3/2,3/3,3/+

The subcategories or minor categories are represented by fractional symbols. The number before the slash mark represents the major category of the ILO Standard that the radiograph most closely resembles. The number after the slash mark represents the major category of the ILO Standard that it next most closely resembles and that was also seriously considered. If the radiograph so closely matches one ILO Standard that no other is seriously considered, the same major category number is recorded before and after the slash. Since the ILO Standards represent the midpoints of the major categories, they more specifically represent minor categories **0/0**, **1/1**, **2/2** and **3/3** and are so identified. To classify a radiograph **2/2** means that it so closely matched the ILO **2/2** Standard that no other Standard was considered. To classify a radiograph **2/1** means that it most closely resembled the ILO **2/2** Standard, but that the ILO **1/1** Standard was also seriously considered. In other words, the profusion of small opacities in the subject radiograph lies on the continuum between the midpoint of major category **1** and the midpoint of major category **2**, but it is closer to **2** than to **1**.

The assessment of profusion by placing the subject radiograph between ILO Standards does not apply at the extremes of the continuum. **0/-** represents obvious, unequivocal absence of small opacities (the “cold normal”), whereas in **0/0**, the midrange of major category **0**, a few equivocal small opacities may be present. At the other end of the continuum, any profusion greater than that represented by ILO **3/3** Standard is indicated by **3/+**.

Profusion should be assessed separately for each of the six lung zones. When you evaluate the profusion of small opacities within a lung zone, consider the total number of small opacities present. If more than one type of small opacity is present, they must all be considered in matching the zone with the ILO Standards for profusion. If small opacities are not uniformly distributed throughout a lung zone, you must estimate what the profusion would be if they were uniformly distributed. Since the report form permits only one expression of profusion, and since profusion often differs from one lung zone to another, the assessments of individual lung zones must be integrated (subjectively averaged). In integrating these values, lung zones that are uninvolved and any lung zones in which the profusion is three or more minor categories less than that of the zones of principal involvement should be discounted. In short, the integrated expression of profusion represents a statement of **average** profusion in only those lung zones that are significantly involved. It does not necessarily represent an average of the profusion of small opacities throughout the whole of both lungs.

Compare each lung zone of the subject radiograph with the ILO midrange standards. Check the box in the "profusion" block that best represents the overall integrated profusion of small opacities in the lungs using the conventions defined above.

1. Include all shape/size small opacities in your judgment of profusion, not just the primary type.
2. Estimate profusion assuming the opacities were evenly distributed in a lung zone, ignoring any lung zones that are uninvolved.
3. Ignore any lung zones in which the profusion of small opacities is 3 or more minor categories less than in the principally involved zones.

Radiograph #4 (images A, B, C and D) illustrates a normal and the typical appearance of midrange, or approximate midrange, profusions for each major category of small opacity **p**.

Radiograph 4A is normal.
Radiograph 4B shows a good example of p opacities at profusion 1/1 in the right upper quadrant (RUQ) between the 2nd and 4th anterior interspaces. Note the A large opacity in the right upper zone.
Radiograph 4C shows a good example of p opacities at 2/2 profusion.
Radiograph 4D shows an example of 3/3 p/p.

Similarly, **Radiographs #5** through **#7** illustrate the typical midrange profusions for primary small opacities **q, s,** and **t.** Note, u opacities **Radiograph #8** are quite rare, therefore the ILO 2011D analog standard is shown **(Radiograph #8b),** along with one example of u opacities in **Radiograph #8c**. As the major category increases from **1** to **2** to **3** the vascular pattern of the lung becomes progressively less distinct. Thus, the degree of vascular clarity may be of assistance in deciding the major category of profusion.

Radiograph #5

Radiograph 5A – Normal.
Radiograph 5B – 1/1 q/q.
Radiograph 5C- 2/2 q/q.
Radiograph 5D – 3/3 q/q especially in the right upper zone (RUZ)

Radiograph #6

Radiograph 6A – Normal.
Radiograph 6B – 1/1 s/s.
Radiograph 6C – 2/2 s/s.
Radiograph 6D – 3/3 s/s.

Radiograph #7

Radiograph 7A- Normal.
Radiograph 7B – 1/1 t/t.
Radiograph 7C – 2/2 t/r.
Radiograph 7D – 3/3 t/s.

Radiograph #8

Radiograph 8A is normal.
Radiograph 8B demonstrates the range of profusion of u opacities using the prior ILO analog standard
Radiograph 8C demonstrates examples of r/r opacities at profusion 1/1 and is the ILO standard radiograph for r/r 1/1. Note there are a very few opacities that are somewhat irregular in shape in the LUL. These are u-type opacities.

Radiograph #9 demonstrates the continuum of minor categories of profusion from **1/1** through **3/+** for small opacity **r**. Note that the distinction between minor categories **0/1** and **1/0** is not illustrated here. This is a somewhat difficult task and is the subject of Subset 4.

Radiograph #9

Radiograph 9A is r/r 1/1.
Radiograph 9B is r/r 2/2.
Radiograph 9C demonstrates r/r 3/3 in the right lung, r/r 3/+ in the left lung. Note the example of a category A opacity right upper zone and coalescence of small opacities (**ax** symbol) in the left upper zone (LUZ).

Radiograph #10

Radiograph 10 was removed from the syllabus.

2C. Large Opacities (Radiographs #11 to #14)

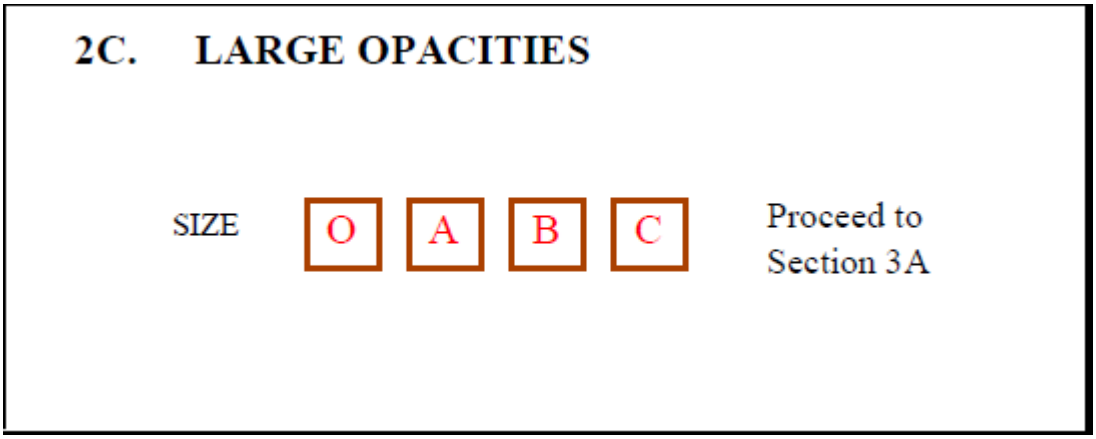

A **large opacity** has a longest dimension greater than 10 mm. Large opacities are classified individually and collectively as follows:

A = An opacity whose greatest diameter exceeds 10 mm but is less than 50 mm, or several opacities each of which exceeds 10 mm in diameter, but the sum of whose greatest diameters does not exceed 50 mm.

B = A large opacity whose greatest diameter exceeds 50 mm but whose area is not greater than the area of the right upper zone, or several large opacities the sum of whose greatest diameters exceeds 50 mm, but which when summed do not exceed an area equivalent to that of the right upper zone.

C = A large opacity whose area exceeds that of the right upper zone, or several large opacities whose areas when summed exceed the area of the right upper zone. Identification of a large pneumoconiotic opacity may be facilitated by recognition of a coexistent background of small pneumoconiotic opacities.

Radiograph #11

Radiograph #11 through **Radiograph #14** demonstrate large pneumoconiotic opacities. **Radiograph #11** is quality "2" due to mottle and shows an **A** 12-mm opacity underlying the right third anterior rib. There is coalescence of small opacities **ax in the right upper lobe**. There are coexistent background small pneumoconiotic round opacities **r/q** involving all lung fields, profusion **2/2**. Other abnormalities include **ax**, and **hi.**

Radiograph #12

Radiograph #12 demonstrates large opacities that when summed would be categorized as **B** since the sum of their longest dimensions exceeds 50 mm, but the sum of their dimensions does not exceed the area of the right upper zone. For illustration purposes, if only one of these two were present, the individual classifications would be as follows: the large opacity underlying the right second anterior rib would be **A** and the opacity underlying the left first and second anterior ribs is about 50 mm in size or **A.** A poorly defined nodule seen through the heart in the left lower zone could be an additional large opacity. For further review of this image, see **Radiograph #24**.

Radiograph #13

Radiograph #13 presents several large opacities whose summed dimensions exceed the area of the right upper zone and are therefore collectively classified **C.** The large opacities involve the middle and upper lung zones on the left and right. There are coexistent background small pneumoconiotic opacities q/q involving all lung zones, profusion **3/3**. Other abnormalities include **bu**, **di, em, id, and ih.**

Radiograph #14

Radiograph #14 demonstrates a B size opacity in the left upper lobe. Two additional opacities are seen in the RUZ between the second and third anterior ribs and the right infra hilar area overlying the distal end of the anterior right 4th rib. Since together they do not exceed the area of the right upper zone, they should be collectively reported as **large opacities, size B.** The symbol **ax** refers to an area of coalescence of small pneumoconiotic opacities (rounded or irregular) within which the margins of the individual opacities are still identifiable. A true **large opacity** such as the opacity seen in the left apex has a more homogeneous appearance.

The distinction between a large opacity and **ax** coalescent opacities is further illustrated in Subset 4.

If no large opacities are present, check **O** in Section 2C, large opacities. If one or more large opacities are present, check the letter **A, B or C** that best represents the area they would collectively occupy if they were contiguous.

Section 3: Pleural Abnormalities

3A. Any Classifiable Pleural Abnormalities?

3A. ANY CLASSIFIABLE PLEURAL ABNORMALITIES?	YES ☐	Complete Sections 3B, 3C	NO ☐	Proceed to Section 4A

You must check “YES” or “NO”.
If “YES”, complete Sections 3B, 3C, and 3D.
If “NO”, proceed to Section 4.
Before discussing the conventions for reporting pleural abnormalities, please note that these conventions may require you to report in several different blocks (as if they were unrelated findings) the different borders created by what may appear in fact to be simply an extended zone of pleural thickening curving around the convexity of the chest.

3B. Pleural Plaques (Radiographs #15 to #17)

3B. PLEURAL PLAQUES *(mark site, calcification, extent, and width)*

Chest wall	*Site*	*Calcification*	*Extent (chest wall; combined for in profile and face on)* Up to 1/4 of lateral chest wall = 1; 1/4 to 1/2 of lateral chest wall = 2; > 1/2 of lateral chest wall = 3	*Width (in profile only)* (3mm minimum width required) 3 to 5 mm = a; 5 to 10 mm = b; > 10 mm = c
In profile	O R L	O R L	O R → 1 2 3 ; O L → 1 2 3	O R → a b c ; O L → a b c
Face on	O R L	O R L		
Diaphragm	O R L	O R L		
Other site(s)	O R L	O R L		

Circumscribed Pleural Thickening (Plaque)

A circumscribed area of pleural thickening is termed a plaque. Pleural plaques may occur along the right and left hemidiaphragms, on the chest wall, or at other sites. They may be seen along the lateral chest wall ‘in profile’, or may be visible ‘face on’, when present on the anterior or posterior chest walls. These hyaline plaques usually result from thickening of the parietal pleura and when seen in profile appear as soft tissue elevations (sometimes with squared-off borders), often along one or both hemidiaphragms. The presence of plaque and calcification within plaques are recorded separately for the right and left sides.

Pleural plaques may also be seen in other sites, such as the mediastinal pleura in paraspinal or paracardiac locations.

An in-profile plaque may be defined as one whose sharp medial margin is roughly parallel to the lateral chest wall and whose shadow merges with the rib edge and lateral chest wall along most of the length of the plaque. Face-on plaque (**en-face** plaque) usually appears as a rounded or ovoid area of opacity without sharp margination on the frontal chest radiograph. At times, face-on plaque may show a sharp margin but be distinguished from in-profile plaque because its shadow does not parallel the lateral chest wall or appear to merge with the rib edge. Some plaques may present both in-profile and face-on components as they wrap the chest wall.

Radiograph #15A Upper and #15A Lower

Radiograph #15A (Upper and Lower) illustrates the typical appearance of both in-profile and face-on chest wall pleural plaques as well as diffuse pleural thickening.

On the left, the in-profile plaque begins at the level of the 6th posterolateral rib and extends down to the level of the 9th posterolateral rib. Medial to the in-profile plaque on the left are poorly defined areas of increased density representing face-on plaques. Do not confuse the scapula overlap on the left with in-profile plaque.

The right side shows a blunted costrophrenic (CP) angle that, when contiguous with plaque a pleural shadow extending superiorly, defines diffuse pleural thickening. The plaque seen on this radiograph has an in-profile and face-on component.

Other abnormalities include post cardiac surgical changes, a mitral valve replacement, and two artifacts from snaps on the patient's gown.

Radiographic images of pleural plaques may include recognizable areas of calcification as demonstrated in the in-profile plaque on the left (see arrow). The presence or absence of calcification is recorded for all plaques and separately for the right and left hemithoraces. When only calcification is seen, a plaque is also recorded as present at that site.

Radiograph #15B

This image illustrates chest wall face-on pleural plaques, as well as bilateral diaphragmatic plaques, most of which are calcified. Uncalcified plaques are said to be the precursor of calcified plaques. On the right side, there are uncalcified face-on pleural plaques in the areas of the fifth and sixth posterior and lateral ribs. In addition, there are calcified face-on plaques overlying the seventh posterior rib on the right and fifth to eighth posterior ribs on the left. Note the rolled-edge or "holly-leaf" appearance of the calcified face-on plaques. There is also calcification within the soft tissue of the plaques along both hemidiaphragms. Please note that if calcification is identified along the chest wall or hemidiaphragms, the calcification may be consistent with that occurring within a plaque even though the soft-tissue component of the plaque is not seen. In this situation, Section 3B should be filled out to indicate the presence of both plaques and calcification. Scoliosis should be recorded under 4A, "Any other abnormalities" and in the appropriate checkbox in Section 4C or as a comment in Section 4E.

Radiograph #15C

This image illustrates left-sided calcified face-on pleural plaques between the eighth and ninth posterior ribs, calcified in-profile plaques along the left lateral chest wall within the same area, and right-sided calcified face-on plaque in the area of the eighth and ninth posterior ribs. There is also blunting of the left costophrenic angle (Section 3C) but no diffuse pleural thickening (Section 3D). Other abnormalities include **ca** in the right upper zone, which must prompt notification of the worker's personal physician.

Radiograph #15D

This image illustrates calcified left-sided chest wall pleural plaques both in profile and face on. The total plaque extent is designated as **2** and the width of the in-profile component is **b**. There is also blunting or obliteration of the right costophrenic angle with an in-profile extension, which is classified as diffuse pleural thickening (see below), but no calcification or face-on component is identified. Bilateral calcified diaphragmatic plaques are noted as well. If a soft-tissue pleural plaque or calcification presumed to lie within such a plaque is identified, check the appropriate box **R** or **L** to indicate its location. If the finding is bilateral, check both **R** and **L.** If no pleural plaque (or calcification) is identified at any site, check **O.** When completing Section 3B of the classification form, you must mark at least one of the three boxes (**R** and/or **L**, or No).

The calcified soft-tissue shadow with sharp inner margins seen along the lower lateral chest wall on the right in **Radiograph #16** represents in-profile plaque extent 1.

Radiograph #17A represents in-profile and face on plaques.

Radiograph #16 and Radiograph #17A

In-profile plaques are classified in terms of extent and presence of calcification, and are required to have a minimum width of 3 mm. Further classification of width is not required but guidelines are given if detailed measurement of width is required for a particular study.

Face-on plaques along the anterolateral/anterior or posterolateral/posterior chest walls are not classified in terms of width. Their extent is approximated and summed with the extent of the in-profile plaque (see below).

Extent. The extent of plaque involvement, noted as **1**, **2**, **3**, is defined in terms of the vertical length of plaque in relation to the length of the lateral chest wall from costophrenic angle to lung apex. If only one in-profile or face-on plaque is present, vertical length is the length of that plaque in relation to the length of the lateral chest wall. If several in-profile or face-on plaques are present in the same hemithorax, vertical length refers to the sum of the lengths of all plaques present in that hemithorax, as described in the ILO guidelines document. Extent is classified as follows:

1 = Total vertical length of plaque (sum of all plaques present, both in-profile and face-on) equal to one-fourth or less of the vertical length of the lateral chest wall.

2 = Total vertical length of plaque (sum of all plaques present, both in-profile and face-on) greater than one-fourth and up to one-half the vertical length of the lateral chest wall.

3 = Total vertical length of plaque (sum of all plaques present, both in-profile and face-on) greater than one-half the vertical length of the lateral chest wall.

In **Radiograph #16**, the extent of the right-sided in-profile calcified plaque is less than one-fourth of the lateral chest wall, indicating extent **1.**

In **Radiograph #17A**, the extent of in-profile plaque on the right is extent 3 – greater than one half, and on the left is extent 2 - greater than one-fourth but less than one-half of the lateral chest wall. Additional face-on plaques are visible as ill-defined hazy opacity overlying the anterior third through sixth ribs. The face-on opacity on the left is partially well-defined laterally and medially, but ill-defined superiorly and inferiorly. The summed extent of the right-side plaques is greater than one-half the vertical length of the lateral chest wall, extent **3.** The face-on plaques in the left hemithorax of **Radiograph #17A** are visible as partially well-defined hazy opacity overlying the second through sixth anterior ribs. A plaque overlying the anterior second rib is well-defined laterally but does not blend in with the lateral chest wall, so it does not constitute a profile plaque. The summed extent of these plaques is greater than one-half the lateral chest wall, extent **3.** Calcification attenuation is visible in the face-on plaques on the left with some linear well-defined densities. A check is placed in the **L** box on the “Face-on” line under “Calcification” in Section 3B.

Width. The width of in-profile plaque is measured as the maximum distance from the inner rib margin along the lateral chest wall to the sharp inner margin of the plaque. Depending on the purpose of the radiograph, recording the width may not be required. Face-on plaques are not classified in terms of width.

The sharp inner margin of the plaque is not necessarily in the same coronal plane as the inner margin of the rib at the lateral chest wall. The 2022 Classification requires a minimum width of 3 mm for in-profile pleural plaque or thickening to be recorded as present. Further classification of width may be performed if required for a particular study. The width of in-profile plaque may then be designated as follows:

a = Maximum width of at least 3 mm up to 5 mm
b = Maximum width over 5 mm and up to 10 mm
c = Maximum width over 10 mm

Therefore, the maximum width for the in-profile plaque on the left in **Radiograph #16** is **b**.

3C. Costophrenic Angle Obliteration

3C. COSTOPHRENIC ANGLE OBLITERATION	R L	Proceed to Section 3D	NO	Proceed to Section 4A

Costophrenic angle obliteration should not be confused with the normal muscle slip attachments of the diaphragm. It is of special relevance in asbestos-exposed people, but it frequently occurs, at least unilaterally, in those not exposed to asbestos or other dusts. Accordingly, minimal costophrenic angle blunting should not be reported.

The ILO 2022 Standard Radiograph labeled CP Angle illustrates the lower limit of costophrenic angle obliteration that should be recorded. Therefore, the appearance of the right costophrenic angle seen in **Radiograph #15C** should not be recorded, whereas that seen in **Radiograph #15D** should be recorded.

If costophrenic angle obliteration is present, whether associated with diffuse pleural thickening of the chest wall or diaphragm, check **R** or **L** or both to indicate its anatomic distribution. If none is present, check "NO" and proceed to Section 4A. By convention, diffuse pleural thickening should be recorded in a hemithorax only in the presence of, and in continuity with, obliteration of the costophrenic angle. If pleural thickening obliterates the costophrenic angle and involves the chest wall, the costophrenic angle obliteration and the upward extension of thickened pleura should each be classified as explained below (see Section 3D).

3D. Diffuse Pleural Thickening (Radiographs #18 to #19)

3D. DIFFUSE PLEURAL THICKENING *(mark site, calcification, extent, and width)*			
Site	*Calcification*	*Extent (chest wall; combined for in profile and face on)*	*Width (in profile only)* (3mm minimum width required)
Chest wall		Up to 1/4 of lateral chest wall = 1	3 to 5 mm = a
In profile O R L	O R L	1/4 to 1/2 of lateral chest wall = 2	5 to 10 mm = b
Face on O R L	O R L	> 1/2 of lateral chest wall = 3	> 10 mm = c
		O R: 1 2 3 — O L: 1 2 3	O R: a b c — O L: a b c

Diffuse pleural thickening is seen in many non-pneumoconiotic disease processes and likely represents thickening of the visceral pleura. Similar to plaque, diffuse pleural thickening may occur in profile or face on. The term "diffuse" indicates a homogeneous involvement to produce a "general veiling of lung parenchymal detail".

If diffuse pleural thickening is seen along the inner margin of the lateral chest wall in continuity with an obliterated costophrenic angle and as a homogeneous shadow, sharply outlined medially by adjacent lung, the thickening is then categorized as in profile. A minimum width of about 3 mm is required for in-profile diffuse pleural thickening to be recorded. On the frontal radiograph, diffuse pleural thickening involving the anterior chest wall may partially obscure lung detail or “veil” the lung. When this veiling is seen, the diffuse pleural thickening is categorized as face on.

When present, diffuse pleural thickening is recorded separately for the right and the left hemithorax. Place a check in the appropriate blocks in 3D for both in profile and face on components. If none is present, check **O.** If diffuse pleural thickening is present, check **R** or **L** or both to indicate its distribution. If **R** or **L** is checked, there must also be a check in each of the remaining boxes in the section. For example, mark **O** if calcification is absent on both sides, and indicate the presence, extent, and width (if required) of the pleural thickening on each side.

Conventions for classifying extent and width are identical for localized plaque and diffuse pleural thickening. Mark **1, 2,** or **3** and **a, b,** or **c** as appropriate to describe the diffuse pleural thickening identified.

Pleural thickening along the chest wall may be circumscribed (plaque, recorded in 3B) or diffuse (recorded in 3D). To distinguish chest wall plaques from diffuse pleural thickening, it is helpful to remember that plaque tends to spare the apex and costophrenic angle, whereas by ILO Guidelines, diffuse thickening must involve the costophrenic angle. The minimum width of in-profile plaque or diffuse pleural thickening to be recorded is 3 mm.

Radiograph #17A shows these normal apical pleural shadows (arrowheads), which often are symmetric and thickest between the lateral first and second ribs. Similarly, one should be careful not to confuse normal symmetrical apical subpleural fat densities, when visible, with pleural thickening. Significant thickening of the apical pleura should not be recorded in Section 3 but should be checked in Section 4B (see below) under **at.**

In **Radiograph #17B,** note that the muscles produce soft-tissue densities frequently oriented obliquely from top to bottom in a lateral-to-medial direction (arrows). One should be careful not to confuse the normal muscle shadows with pleural plaques.

Radiograph #15D shows another example of diffuse pleural thickening on the right. It may be a result of asbestos exposure but is less specific than plaque and may also occur along the hemidiaphragm. When it does, there is coexistent costophrenic angle obliteration. This diffuse pleural thickening along the hemidiaphragm may cause the hemidiaphragm to appear ill-defined. If this loss of definition involves more than one-third of the affected hemidiaphragm, the symbol **id** in Section 4B should be checked.

The width and extent of in-profile diffuse thickening and the extent of face-on diffuse thickening are measured as described above, similar to pleural plaque. The diffuse pleural thickening seen in profile along the right lower lateral chest wall is of width **a** and of extent **2.**

In **Radiograph #18A**, in-profile diffuse pleural thickening along the right lower lateral chest wall is of width **b** and of extent **2.** The right lower and middle zones in **Radiograph #18A** and **#18B** demonstrate a veiling appearance of diffuse thickening face on. In **#18B**, the extent is **2** and width **b** on the right and extent **2** and width **b** on the left.

Radiograph #18A and Radiograph #18B

Pleural thickening, whether circumscribed or diffuse, may be seen only in profile, only face on, or in combination. Each form of pleural thickening that is seen should be separately recorded, even though it may appear that these different forms, in fact, represent a single extended zone of pleural thickening seen in a variety of projections.

Remember the rule distinguishing localized plaque from diffuse pleural thickening: plaque spares the apex and costophrenic angle (**Radiograph #17A**); diffuse pleural thickening involves the costophrenic angle (**Radiograph #18A**). Lastly, it should be emphasized that it is common to see unequivocal plaque formation in the absence of small parenchymal pneumoconiotic opacities (**Radiograph #17A**).

Pleural calcification may be seen with exposure to asbestos but may also be secondary to trauma or old infection. The calcification associated with pneumoconiosis is more often bilateral than unilateral. Unilateral pleural calcifications should be classified as pneumoconiosis (Radiograph #16); however, one may note other etiologies in the comments section if they are suspected. One should search for other findings indicative of pneumoconiosis before attributing unilateral pleural calcification to a pneumoconiotic process. If pleural calcification is linear, it is relatively easy to recognize. It may be discontinuous and may appear in the form of punctate opacities or spicules, making recognition more difficult. In particular, punctate or spiculated calcification seen in face-on plaques may be confused with small pneumoconiotic opacities or calcified granulomas. Large plaques containing marginal calcification may appear to have rolled edges and have been likened in appearance to holly leaves or candle wax.

Hemidiaphragmatic calcification is seen in **Radiograph #15B.**

In **Radiograph #19**, extensive diffuse pleural thickening is present on the left. Note the obliteration of the left costophrenic angle and the veiling of the left lower lung zone.

Radiograph #19

In **Radiograph #19**, the face-on pleural plaque demonstrates calcifications. On the right, the pleural process is diffuse with extent 3 and the width is **c**. Face-on and in-profile plaque with calcification is seen on the left, Note, do not confuse scapula overlay with pleural shadows.

Section 4: Any Other Abnormalities

4A. Any Other Abnormalities

4A. ANY OTHER ABNORMALITIES?	YES ☐ Complete Sections 4B, 4C, 4D, 4E	NO ☐ Complete physician info and sign form.

If "NO", proceed to Section 5. If "YES", complete Sections 4B, 4C, 4D, and 4E.

4B. Other Symbols (Obligatory)

Certain important radiographic findings may be recorded by using symbols. The term "obligatory" implies that if any of the findings represented by the symbols listed are present, the appropriate symbol must be checked. Each of the following definitions may be preceded by the word or phrase "suspect", or "changes suggestive of".

4B. OTHER SYMBOLS (OBLIGATORY)

aa at ax bu ca cg cn co cp cv di ef em es fr hi ho id ih kl me pa pb pi px ra rp tb

aa atherosclerotic aorta
at significant apical pleural thickening
ax coalescence of small opacities - with margins of the small opacities remaining visible, whereas a large opacity demonstrates a homogeneous opaque appearance - may be recorded either in the presence or in the absence of large opacities
bu bulla(e)
ca cancer, thoracic malignancies excluding mesothelioma
cg calcified non-pneumoconiotic nodules (e.g. granuloma) or nodes
cn calcification in small pneumoconiotic opacities
co abnormality of cardiac size or shape
cp cor pulmonale
cv cavity
di marked distortion of an intrathoracic structure
ef pleural effusion
em emphysema
es eggshell calcification of hilar or mediastinal lymph nodes
fr fractured rib(s) (acute or healed)
hi enlargement of non-calcified hilar or mediastinal lymph nodes
ho honeycomb lung
id ill-defined diaphragm border - should be recorded only if more than one-third of one hemidiaphragm is affected
ih ill-defined heart border - should be recorded only if the length of the heart border affected, whether on the right or on the left side, is more than one-third of the length of the left heart border
kl septal (Kerley) lines
me mesothelioma
pa plate atelectasis
pb parenchymal bands - significant parenchymal fibrotic stands in continuity with the pleura
pi pleural thickening of an interlobar fissure
px pneumothorax
ra rounded atelectasis
rp rheumatoid pneumoconiosis
tb tuberculosis

Symbol	Definition
aa	Atherosclerotic aorta.
at	Significant apical pleural thickening.
ax	Coalescence of small pneumoconiotic opacities (discussed and illustrated in Subset 4).
bu	One or more bulla(e).
ca	Cancer of the lung. If one considers that a large opacity might be due to pneumoconiosis but might equally well represent a malignancy, then Section 2C LARGE OPACITIES should be completed, the symbol "ca" should also be checked, and an appropriate comment should be written in Section 4D. If one believes that a large opacity truly represents a malignancy and is not a manifestation of pneumoconiosis (as might be the case in the absence of small pneumoconiotic opacities), "ca" should be checked. However, Section 2C LARGE OPACITIES should not be completed, and a comment stating where the malignancy is seen should be entered in Section 4D. Pleural mesothelioma is not recorded here but rather as “me" (see below).
cg	Calcified non-pneumoconiotic nodules (e.g. granuloma) or hilar/mediastinal lymph nodes.
cn	Calcification in small pneumoconiotic opacities (not to be confused with calcified granulomas).

co	An abnormality of the cardiac size or shape.
cp	Cor pulmonale.
cv	Cavity
di	Marked distortion of intrathoracic organs (see elevated left hilum in Radiograph #14).
ef	Pleural effusion.
em	Emphysema.
es	Eggshell calcification of hilar or mediastinal lymph nodes.
fr	Fractured rib (s) (acute or healed).
hi	Enlargement of non-calcified hilar or mediastinal lymph nodes.
ho	Honeycomb lung (see Radiograph #7, t/t - 3/3).
id	Ill-defined diaphragm (if more than one-third of one hemidiaphragm is involved).
ih	Ill-defined heart outline (if the length of the heart border affected, whether on the right or on the left side, is more than one-third of the length of the left heart border.)
kl	Kerley lines, septal lines (See Radiograph #6, s/s - 3/3).
me	Mesothelioma.
pa	Plate atelectasis.
pb	Parenchymal bands (significant parenchymal fibrotic strands in continuity with the pleura).
pi	Pleural thickening of an interlobar fissure (a thickened minor fissure is seen in Radiograph #6, s/s - 3/3).
px	Pneumothorax.
ra	Rounded atelectasis.
rp	Rheumatoid pneumoconiosis.
tb	Tuberculosis (excluding the calcified primary complex).

Some of these symbols are illustrated in this subset; others are illustrated in subsequent material.

Check all appropriate boxes in **Section 4B**.

The symbols in Section 4B do not encompass all possible abnormalities potentially present in a chest radiograph. If findings are present other than those represented by the symbols found in Section 4B, or if further description or discussion of the findings is needed, then make entries as appropriate in sections 4C and/or 4E. If you are the first reader, please notify the worker or his or her physician and enter the date of such notification in the blocks to the right in Section 4D.

Sections 4C, 4D, and 4E*

4C. MARK ALL BOXES THAT APPLY: (Use of this list is intended to reduce handwritten comments and is optional)

Abnormalities of the Diaphragm

- ☐ Eventration
- ☐ Hiatal hernia

Airway Disorders

- ☐ Bronchovascular markings, heavy or increased
- ☐ Hyperinflation

Bony Abnormalities

- ☐ Bony chest cage abnormality
- ☐ Fracture, healed (non-rib)
- ☐ Fracture, not healed (non-rib)
- ☐ Scoliosis
- ☐ Vertebral column abnorma

Lung Parenchymal Abnormalities

- ☐ Azygos lobe
- ☐ Density, lung
- ☐ Infiltrate
- ☐ Nodule, nodular lesion

Miscellaneous Abnormalities

- ☐ Foreign body
- ☐ Post-surgical changes/sternal wire
- ☐ Cyst

Vascular Disorders

- ☐ Aorta, anomaly of
- ☐ Vascular abnormality

Date Physician or Worker notified? (mm-dd-yyyy)

4D. Should worker see personal physician because of findings? YES ☐ NO ☐ ☐☐-☐☐-☐☐☐☐

4E. OTHER COMMENTS

These sections are used to record information about the classification of the radiograph. They focus on other causes thought to be responsible for a finding that might be secondary to pneumoconiosis, radiographic findings of possible significance not noted above, and any further explanatory comments deemed appropriate. If it is deemed important for the worker to see his or her physician because of findings reported in this section, for follow-up, or for comparison of the current study with previous radiographs, check **"YES"** in the box at the bottom of Section 4D. If not, check **"NO."** If you are the first reader to classify an image, you should ensure that the worker or the physician is notified of any clinically significant findings.

NOTE: Section 4C intends to reduce the need for handwritten comments in Section 4E, while facilitating accurate recording and coding of common abnormalities. It is optional.

*You may encounter minor differences between classification forms due to periodic revisions. However, the most significant components of the forms, and most importantly, the principles of classification, remain unchanged.

Section 5

Reader's Initials. Date of Reading.

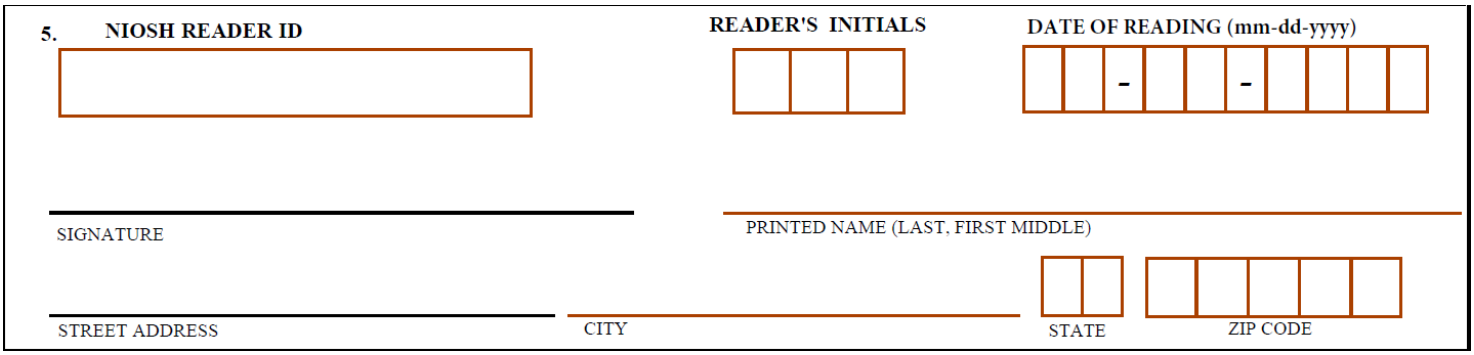

This section provides information for identifying the physician who is interpreting the radiograph.

If appropriate, enter your NIOSH Reader ID.

Then, enter your initials and the date of your reading in the blocks provided. Record your last name and address in the blank spaces.

SUBSET 2 – Radiograph #20 to #27

Reminder: The PDF portfolio of answer keys is a separate PDF portfolio.

Radiograph #20

This radiograph is from a coal miner. Initial evaluation shows small, rounded opacities and large opacities. Detailed analysis then proceeds through the following sequence of decisions.

Radiograph quality is graded 2 due to scapula overlay. The parenchymal opacities are consistent with pneumoconiosis, so Section 2A is checked "YES."

The primary small opacity is rounded and estimated to be of the **q** size (1.5 to 3.0 mm in diameter). The secondary small opacity is of the **r** size (3 to 10 mm). All zones are involved. A comparison of the radiograph with the ILO standards shows the closest match to be the q/q - 2/2 standard, although a match with q/q – 1/1 is also a consideration. Thus, Section 2B is classified as **q/r**, both upper and middle zone involvement, with a profusion of **2/1**.

The right upper zones overlapping the first, second, and third anterior ribs show well-defined large opacities. These constitute a **B** large opacity; that is, the sum of the greatest dimensions of the large opacities is greater than 5 cm.

There are no pleural plaques and the costophrenic angles are not blunted, so the “NO” box is checked in 3A.

Other abnormalities are present, so in 4A the “YES” box is checked. The symbol **di** for distortion **em** for emphysema.

Radiograph #21

This radiograph, on initial inspection, appears to show parenchymal and pleural abnormalities consistent with asbestos exposure. Detailed analysis would follow a pattern of sequential decision-making such as that indicated below.

The technical quality of the radiograph is graded 2, improper position, rotated left anterior oblique (LAO).

The chest shows abnormalities consistent with pneumoconiosis, so Section 2A is checked "YES."

Careful inspection of all zones reveals small irregular opacities and the size and shape are consistent with primary **s** and secondary the definition of **t** opacities. The lower zones are involved. A comparison of the radiograph with the ILO Standard shows the profusion to match most closely with the ILO s/s - 1/1 Standard.

Large opacities are not present.

There are pleural abnormalities consistent with pneumoconiosis, so 3A is checked "YES," and one proceeds to 3B.

Pleural plaques are present bilaterally both in profile and face on, so for 3B chest wall, **R** and **L** are marked for both in profile and face on. Plaque is also visible along the diaphragms and the posterior mediastinum bilaterally, so **R** and **L** are marked for the diaphragm and other site(s). Fine linear calcifications are noted on the left cardiac border. The soft-tissue component of the plaques is not seen along the posterior mediastinum or heart, but their presence is inferred from the calcification. This is also true for some plaques along the hemidiaphragms, which are visible only because of the calcification. The extent of the plaque, combined for both in-profile and face-on plaque, is over one-half the length of the lateral chest wall, so both **R** and **L** are marked as **3.** The maximum width of the in-profile plaque is between 5 and 10 mm, so **b** is marked for both **R** and **L.**

There is no costophrenic angle obliteration and, therefore, no diffuse pleural thickening. The slight pleural thickening at the left costophrenic angle is less than the lower limit for recording costophrenic angle obliteration, which is illustrated on the ILO Standard labeled costophrenic angle blunting (CPa on B-Viewer).

Section 4A is checked "YES" because there are other abnormalities present. Cardiomegaly is present, so **co** is marked. The symbol ca may be checked because of concern for a possible tumor. Sternal wires should be noted under 4C. The patient should be advised to see his or her physician for the cardiomegaly, although this may be chronic. Significant right lower zone atelectasis should be followed-up or evaluated with chest CT.

Radiograph #22

This radiograph is from a man who was previously exposed to asbestos. There are extensive parenchymal and pleural abnormalities consistent with asbestos-related pleuropulmonary disease. A detailed analysis is described below.

The technical quality is classified as **2** because of a slight left anterior oblique rotation and superimposition of the left scapula.

Since there are parenchymal abnormalities, Section 2A is marked "YES."

Small irregular opacities are present in the four lower zones but best seen on the left. The pleural abnormalities partially obscure those on the right. The primary type of opacity is **t**; the secondary is **s.** The profusion, when compared with ILO Standards, is graded 1/2. The Standard Radiograph s/s - 1/1 provides the closest match with a combination of irregular opacities, but the profusion in the left middle and lower lung zones is slightly greater than that in the 1/1 Standard. Therefore, category 2 should be considered as an alternative. Hence, the profusion is recorded as **1** (primary consideration) over **2** (the other level considered). There are no large opacities.

Pleural abnormalities are obviously present on the right; therefore, Section 3A is checked "YES," and Sections 3B, 3C, and 3D are completed because the pleural abnormalities are consistent with those of pneumoconiosis (in this case, asbestos-related disease). The pleural abnormalities are significant and consistent with plaque and diffuse pleural thickening.

Chest wall pleural plaque is seen face on and in profile on the right. There are no pleural calcifications identified. The extent of the plaque is greater than half the vertical length of the lateral chest wall, so the extent on the right is graded 3. The maximum width of the in-profile plaque on the right is about 10 mm and is therefore graded **c.**

Mark **R** in 3C since the right costophrenic angle is blunted in comparison to the CP Angle Standard Radiograph. Although there is face-on pleural plaque, there is no definite diffuse pleural thickening or calcification. The right costophrenic angle is blunted and the pleural thickening does not extend up the lateral chest wall. Keep in mind that the pleural thickening on the lateral chest wall must exceed 3 mm to be recorded. Note the separation of the blunted angle and the pleural plaque more superiorly on the right lateral chest wall.

There are other abnormalities present; therefore, Section 4A is checked “YES.” In Section 4B, **aa** is checked because of calcification of the aortic arch. A loss of definition of the right diaphragm is indicated by checking **id** and **fr** for an old rib fracture noted in the left 7^{th} and 8^{th} lateral rib.

Radiograph #23

This case demonstrates pleural plaques and pleural effusion without small parenchymal opacities. In many instances, pleural abnormalities are the first radiographic evidence of asbestos exposure. A detailed analysis is described below.

The technical quality of the radiograph is classified as 3 because of overexposure of the lungs, and “Overexposed (dark)” is checked. Other technical deficiencies include improper position (because the scapulae overlap the lungs) and exclusion of the left costophrenic angle, which is included in a second image. Artifacts, perhaps monitors, are also present.

No parenchymal abnormalities are consistent with pneumoconiosis, so "NO" is checked in Section 2A.

There are extensive pleural abnormalities bilaterally involving the chest wall and both costophrenic angles. Section 3A is therefore checked “YES.”

There are in-profile and face-on pleural plaques on the left lateral chest wall, so in 3B, “in profile” and “face on” are marked **L** for Site. Pleural calcifications are visualized in these plaques, so in profile and face on are marked **L** under Calcification as well. The left chest wall plaques are classified as follows: on the left, the maximum width of the plaque (the distance from the medial surface of the adjacent rib to the most medial and sharpest margin of the circumscribed plaque) measures more than 10 mm (width **c**). The combined length is between one-fourth and one-half of the projection of the lateral chest wall, classified as extent 2. (The face-on component produces a less sharply defined border overlying the third through fifth ribs anteriorly.) No right face-on or in-profile plaque exists, so **O** is marked under extent and width for the right side.

The right and left costophrenic angles are blunted by thickened pleura or effusion. The left is seen on the second lower image of the chest., so Section 3C is checked **R,** and **L.** Diffuse pleural thickening usually extends into and obliterates the entire costophrenic angle. This is the case on the right; however, the left CP angle blunting is not continuous with the left chest wall in profile or face on process. Therefore, this is not classified under diffuse pleural thickening. On the right, the diffuse pleural thickening is seen both in profile and face on, and the findings are recorded in 3D as **R** for “Chest wall, Site.” There is no in-profile or face-on diffuse pleural thickening on the left. There is calcification of the diffuse pleural thickening on the right seen face-on, so **R** is marked under Calcification for face-on plaque but not for in-profile plaque. The length exceeds one-fourth of the lateral chest wall but is less than half, so it is classified as extent **2,** whereas the width is greater than 10 mm and is therefore classified as **c.** There is no left diffuse pleural thickening, so **O** is marked under extent and width for diffuse pleural thickening on the left side.

Section 4A is checked “YES” to indicate that other abnormalities are present. These are indicated as follows: a pleural effusion may be present, so **ef** is checked; there may possibly be a mesothelioma on the right, so **me** is appropriately checked. (However, a mesothelioma usually produces an extensive pleural effusion and pleural nodularity, so the diagnosis is not likely in this case.) Notation should be made under 4C of the post-surgical changes of cardiac surgery and sternal wires. Since **me** was considered, the worker’s personal physician should be notified.

Radiograph #24

On initial inspection, this individual appears to have characteristic findings of silicosis and its sequelae. However, CWP may have the same appearance and it is usually impossible to differentiate the two conditions. Large opacities are obvious in both lungs, more marked on the right. To differentiate pneumoconiosis from other diseases, such as sarcoidosis or tuberculosis, one must search for associated findings that are almost always present in advanced pneumoconiosis. The most important include small rounded or irregular opacities, distortion of the intrathoracic organs because of retraction toward the conglomerate masses, compensatory emphysema, and eggshell calcification in hilar or mediastinal lymph nodes. In this case, a pattern of small opacities is seen throughout both lungs, so the findings are consistent with pneumoconiosis. The case should be classified as follows:

The technical quality is good and is therefore classified as **1**.

Since there are parenchymal abnormalities consistent with pneumoconiosis, 2A is marked "YES."

Small, rounded opacities are present. Those whose shape and size correspond to the definition of **q** opacities (more than 1.5 mm but less than 3 mm in diameter) predominate, so **q** is marked as the primary opacity type. However, a number of opacities have diameters greater than 3 mm, so **r** is checked as the secondary type of small opacities. It is useful to compare the appearance of the small, rounded opacities with the ILO Standards to confirm this classification with respect to size and shape.

All six lung zones are involved.

Comparison of the radiograph with the ILO Standards shows that the profusion of small opacities corresponds so well with the q/q - 1/1 Standard that no other Standard needs to be considered. The profusion is, therefore, 1/1. The profusion was probably greater before the development of the large opacities and the compensatory emphysema. It is believed that multiple small opacities become incorporated into the mass, thus decreasing the apparent level of profusion.

The large opacities have a combined area less than the area of the right upper lung zone, and the sum of their diameters exceeds 5 cm. Therefore, they are classified as **B.** A poorly defined, possible additional large opacity is seen through the heart in the left lower zone.

There are no pleural abnormalities consistent with pneumoconiosis.

Other abnormalities include **aa, ax, ca**, **em**, and **tb**.

Radiograph #25

An example of **ax** is seen in the right first anterior interspace overlapping the right second anterior rib at its midportion. The small, rounded opacities making up this **ax** have identifiable margins, unlike the more homogeneous appearance of the large opacities that are also present. The large opacities seen are consistent with those of pneumoconiosis since a background of small opacities is also present. The prominent left hilum is appropriately indicated with the symbol **hi. Symbols ca and di are also checked.**

Radiograph #26

Normal intercostal muscle shadows are well illustrated in this radiograph and should not be confused with pleural plaque. Note the slightly obliquely-oriented soft-tissue margins best seen over the right anterolateral 6th and 7th ribs.

Radiograph #27

The exam is quality 1 and shows examples of **ax** in the upper zones bilaterally (short arrow), where small opacities demonstrate coalescence as there are identifiable margins for the small opacities. The opacities are r/q in size and shape present in all zones at a profusion of 3/2. There are also size **A** large opacities (long arrows) arising near the peripheral margins of both upper zones. Their combined longest dimensions suggest a size **B** classification. Note that the symbol **di** should be checked due to a loss of volume in the right and left upper lobes. Symbol **hi** should also be checked to indicate right hilar enlargement.

SUBSET 3 – Radiograph #28 to #38

Reminder: The PDF portfolio of answer keys is a separate PDF portfolio.

Radiograph #28

With a background of small pneumoconiotic opacities, the large opacity in the right upper/middle zone is consistent with a size A large opacity of pneumoconiosis (PMF, conglomerate mass). If you are concerned that this might possibly represent a carcinoma, it should be recorded as **ca** in 4B and the "Other Comments" Section 4D, as shown on the reporting form 28. Please note that if a lesion is also consistent with PMF, **ca** alone is not correct. In Section 4B, **ax** and **di** were also selected. Hilar adenopathy is also likely and designated by **hi.**

Radiograph #29

This is an example of image quality **2,** since the left arm is superimposed over the left lateral chest wall, which could be mistaken for pleural thickening. Mottle was also noted. This radiograph illustrates a combination of small, rounded opacities, primarily **r** and, secondarily irregular opacities **t.** The profusion 2/2 represents a subjective average of the profusions found in the upper and middle zones since the profusion of small opacities in the middle and upper zones is greater than two small categories more profuse than in the lower zones. Therefore, while all zones are checked denoting the presence of small opacities, the lower zones are excluded from averaging. Note the poorly defined densities at the right fifth and seventh posterior ribs and at the left eighth posterior rib, reflecting callus formation at healed fracture sites. They should not be mistaken for large opacities and should be recorded in Section 4B as **fr.**

Radiograph #30

Several large opacities are present. Their areas, when summed, exceed the area of the right upper lung zone; therefore, they are recorded as size **C** in Section 2C. There are no pleural abnormalities. In Section 4B, **ax, bu, di, em, id, hi,** and **ih** were selected.

Radiograph #31

As small pneumoconiotic opacities become incorporated into large opacities, the apparent profusion of small opacities may decrease. Note their relatively low profusion (1/2) in this patient. Large opacities are present bilaterally, which when summed, correspond to size C. In-profile plaque is clearly present on the left, extent 3, width b, with parenchymal bands visible bilaterally. This raises the possibility that some of the large opacities could represent face-on plaque. A comment could be added in Section 4C suggesting that further evaluation with CT might be required to distinguish between them. The appearance of the right CP angle does not reach the degree of blunting necessary to classify it.

Radiograph #32

Again, the profusion of small opacities is low in the presence of large opacities classified as **B.** Note the distortion of the right hilum, **di,** a finding sometimes associated with large opacities. Symbols **aa, at, ax, di, em, hi,** and **pi** are checked.

Radiograph #33

Note that large opacities may occur in the middle and lower lung zones. The combined long axis diameter is greater than 5 cm, so category B is checked under 2C. The symbol for a rib fracture (**fr,** posterolateral right ninth) should be checked for this image. Concern for malignancy was raised regarding the large opacity on the right and **ca** was checked in 4B. The worker's personal physician should, therefore, be notified. Sternal wires should be mentioned in 4C. Symbols **aa, ax,** and **cg** are also checked.

Radiograph #34

In this example, chest wall pleural plaque (in-profile and face-on) is recognized mainly by the presence of calcium. The soft-tissue shadow of the plaque is less apparent. In this circumstance, plaque is presumed to be present, and both the site and calcification must be recorded in Section 3B. Note that the rolled-edge appearance of a calcified face-on plaque is illustrated in the left middle lung zone. Irregular opacities are present in both lower zones, size s/t, profusion 1/1. See the comments on Radiograph # 21 for additional findings.

Radiograph #35

Radiograph #35 demonstrates irregular opacities size s/s in both lower zones at a low profusion but clearly abnormal, graded 1/0. Pleural abnormalities are present bilaterally including in-profile plaques bilaterally, calcified face-on plaque, and diaphragmatic plaque on the left.

Radiograph #36

Bilateral chest wall plaques are present. Note the sparing of the apices and costophrenic sulci. In-profile plaque is noted on the right without calcification. Face-on plaque is noted bilaterally with calcification. Other sites plaque with calcification is visible in the right paraspinal area**.** Extent for both **R** and **L** is **3**; and width is **c** on the right.

Radiograph #37

No small, pneumoconiotic opacities are seen, but definite pleural thickening is present. The plaques on the left spare the costophrenic sulcus and apex (review Subset 1). Face-on and in-profile chest wall plaques with calcification on the left, bilateral calcified diaphragmatic plaque, and paraspinal calcifications ("other sites") should be recorded in Section 3B. Note that the diffuse pleural thickening on the right involves the costophrenic sulcus and extends up the chest wall; it should be recorded in 3C. The extent is **1** and the width is **a,** noting the presence of calcification.

Radiograph #38

Note the extensive, calcified, in-profile and face-on left chest wall plaques that spare the apex and costophrenic angle. There is obliteration of the right costophrenic angle with diffuse pleural thickening. There are no small pneumoconiotic opacities. Note that this image is the ILO standard for blunting of the costophrenic angle. Additional comments are available at Radiograph #15D.

SUBSET 4 – Radiograph #39 to #46 (Small and Large Opacities)

Reminder: The PDF portfolio of answer keys is a separate PDF portfolio.

Subset 4 is a narrative analysis of small rounded and small irregular opacities at profusion levels of 0/1 and 1/0, illustrated by representative radiographs. In addition, the subset includes composite radiographs that illustrate examples of **ax,** large opacity **A,** and carcinoma of the lung.

Small Opacities

The ILO 2022 system classifies the small parenchymal opacities of pneumoconiosis according to shape, size, extent, and profusion or concentration. The correct determination of profusion is important because it is the best-known indicator of the lung's dust burden. Also, although not intended for this purpose, various state and federal agencies have used profusion levels as part of the medical evidence in the adjudication of compensation claims.

Various structures, both normal and abnormal, may produce similar patterns. For example, small blood vessels projected on end commonly appear as small, rounded opacities. Usually, small blood vessels are fewer in number and less uniform in size than pneumoconiotic small opacities, and they are usually associated with the characteristic branching shadows of vessels seen in profile. Also, in the normal aging process, bronchovascular structures may thicken and become irregular, making them difficult to distinguish from the small irregular opacities of pneumoconiosis. This may be more pronounced if the individual has a smoking history, has had repeated pulmonary infections, or shows early manifestations of congestive heart failure. Many other pathologic conditions not related to pneumoconiosis from mineral dust exposure may also present as small opacities in any or all lung zones. Histoplasmosis or varicella are examples.

It has been stated that when the profusion of pneumoconiotic opacities is minimal, there are few situations in diagnostic radiology where the differentiation of the normal from the abnormal is more difficult. The availability of a 12-point scale of profusion for both small rounded and small irregular opacities may appear to indicate that profusion levels are easily distinguished and quantified. Such is not the case, however, particularly at the lower end of the scale, where profusion levels of 0/1 and 1/0 must be differentiated. As a result, inconsistencies occur, and multiple readings may be necessary to resolve differences, even among experienced readers. Several factors are responsible for the inconsistencies of interpretation at these profusion levels. Among these are poor image quality, a lack of experience with chest radiography or the ILO Classification system, and a lack of familiarity with the radiographic appearances of the pneumoconioses.

The ILO Standard Radiographs illustrate only the middle categories of profusion, **0/0**, **1/1**, **2/2**, and **3/3**. This subset is, therefore, specifically designed to familiarize the reader with the distinctions among profusion levels **0/0** (normal), **0/1** (normal), **1/0** (abnormal), and **1/1** (abnormal) as they relate to small opacities of various shapes and sizes.

Now, look at radiographs #39 to #46 in turn and compare each with the narrative description provided. In each of these radiographic series, image A represents a normal lung with profusion **0/0**, and images B, C, and D represent higher levels of profusion of small pneumoconiotic opacities.

Radiograph #39 – Type p

Small rounded opacity of type p

Radiograph #39A represents a normal lung. The normal vascular pattern is well illustrated. There are several small blood vessels seen on end, which should not be confused with small, rounded opacities.

There are **p** and a few **t** small opacities present in **Radiograph #39B**, but they are few at low profusion, appearing as tiny opacities like fine grains of sand. This image represents profusion level **1/0**. The identification of low profusion radiographs is strongly influenced by the quality of the radiograph. Beware of overreading profusion in the presence of grid lines, slight underexposure, extensive overlying soft tissue, or excessive radiographic contrast.

Radiograph #39C. Here, **p** rounded opacities are present at profusion **1/1.** There are many small blood vessels seen on end. Do not confuse end-on vessels with **q** opacities.

Radiograph #39D. Close observation will reveal multiple **p** and a few **s** opacities. This image represents profusion level **1/1**. There is blunting of the right costophrenic angle, but no diffuse pleural thickening is identified. Since there is no pleural abnormality apart from the blunted right costophrenic angle, box 3A is checked "YES," and box 3C checked "YES" for the right; but all other boxes in Section 3B and 3D are checked 0.

Radiograph #40 – Type q

Small rounded opacities, type q

Radiograph #40A. This image presents the absence of small parenchymal opacities, profusion **0/0**.

Radiograph #40B. In this image, the quality is 2 due to significant scapula overlay. Small, rounded opacities of the **q** size are subtly, but clearly, present in the upper zones, but somewhat less profuse than the category **1/1 standard**. In other words, 1/0 profusion.

Radiograph #40C. This radiograph illustrates **q** opacities in the upper zones that are more numerous than in Radiograph #40B above. However, there are still fewer opacities than in the 1/1 q/q standard. This image presents another example of profusion level 1/0.

Radiograph #40D.
This image is quality 2 due to overexposure, mottle, and underinflation. However, one can still clearly see **q** opacities in all zones at profusion level 1/1. Note that a few small opacities in image 40D are slightly larger than those in images 40B and 40C but are all within the defined limits of size for **q** opacities (exceeding 1.5 mm and up to about 3 mm). Hilar adenopathy is likely present and **hi** is checked in Section 4B. There is a 1 cm nodular density at the right base over the 4th anterior rib, possibly a lung nodule or nipple shadow, and should be followed up. Check "YES" for "Should patient see personal physician?" Note partially visible fusion hardware in the lower cervical spine.

Radiograph #41 – Type r

Small rounded opacities, type r

Radiograph #41A. This image presents no small parenchymal opacities, profusion **0/0**.

Radiograph #41B. This radiograph is an example of **r** opacities, few in the upper lung zones, occurring with a profusion of **0/1**. The presence of small opacities is rather subtle. As noted previously, technical limitations may lead to over-reading profusion category 0/1.

Radiograph #41C. Numerous rounded opacities are unequivocally present in all zones of this image at profusion 1/1. The opacities in this radiograph are predominantly **r** opacities but with a few **q** opacities present as well.

Radiograph #41D is a good example of **r** opacities in all zones with relative sparing of the left base, at a profusion of 1/1. Note that the opacities in images #41B, #41C, and #4a1D differ slightly in size, but all fall within the defined limits (3–10 mm) for **r** opacities. The symbol **ax** should be checked to identify the coalescence seen under the right clavicle, first rib crossing.

Radiograph #42 – Type s

Small irregular opacities, type s and t

Radiograph #42A. This image presents no small parenchymal opacities, profusion **0/0**. The hilar shadows, vascular pattern, and pleura are all normal.

Radiograph #42B. The few irregular opacities in this image are **s** irregular opacities, predominately in the lower zones, right greater than left. Remember, **s** irregular opacities measure up to 1.5 mm in width. The vascular pattern here is largely intact. This radiograph presents a profusion level of 1/0.

Radiograph #42C
Radiograph #42C presents more irregular opacities in the lower zones than image #42B and, therefore, has a profusion of 1/1. The vascular pattern is perhaps less distinct, with more irregular opacities in the lateral lower zones. Low-profusion **s** opacities can be difficult to distinguish from normal vascular structures. An attenuation of blood vessels in the upper lobes suggests emphysema. The symbols **aa** and **em** are checked.

Radiograph #42D. This image presents **t** irregular opacities in both middle and lower zones. The vascular pattern is becoming less distinct, especially in the left lower zone and in the periphery of the right lower zone. This image should be classified as t/t 1/1. The obvious pleural disease should be classified, see answer sheet.

Radiograph #43 – Type t

Small irregular opacities type, s and t continued

Radiograph #43A presents no small parenchymal opacities, profusion 0/0.

Radiograph #43B. Type **t** opacities are defined as irregular opacities that are 1.5 to 3 mm wide. There are a few **t** opacities present in both lower zones; however, the right lower zone also presents atelectasis. The vascular pattern is intact in the left lower zone. The image presents a profusion of 0/1. The pleural disease should be classified, see answer sheet. Symbols **aa, cg** and **pb** are also checked.

Radiograph #43C presents a greater concentration of **t** irregular opacities than image #41B. Both middle and lower lung zones are involved. There are fewer opacities in the left base so when averaged this image represents a profusion of 1/0. The vascular pattern is less distinct. Some readers suggested that a calcified right diaphragmatic plaque is present. However, most readers judge it not to be present; therefore, the classification sheet reflects that of most of the readers.

The soft tissue line on the right was not interpreted as intercostal muscle and not pleural plaque. Symbol **aa** is checked.

Radiograph #43D. This image presents t/q opacities at a profusion of 1/1 involving all lung zones bilaterally. The vascular pattern is mildly indistinct. Bilateral pleural involvement with calcification is noted. Face-on plaque, diaphragmatic plaque, and other sites are on the right and left. There is only in-profile plaque on the left. The symbol **aa** for calcifications in the aortic arch is noted.

Radiograph #44 – Type u

Small irregular opacities, type u

U opacities are quite rare. Digital images of low profusion u opacities were not obtained. Please refer to the quadrant images from the ILO 2022 Standards for examples.

Symbol ax

Symbol **ax** refers to an area of coalescence of small opacities. The area may be of any dimension but is not homogeneous in character because the margins of individual small opacities are still identifiable. A large opacity "A" is more homogeneous. It should be noted that coalescence may occur with small rounded as well as with small irregular opacities. Coalescent small opacities (**ax**) and "A" large opacities may be present in the same radiograph and should be so classified. In many instances, superimposition of multiple discrete small opacities may appear as coalescence or even as a large opacity. Additional projections or chest CT would likely resolve the issue. The distinction of whether a shadow represents coalescence vs a large opacity is not trivial; some federal and state agencies consider the presence of a large opacity as evidence of disability.

Radiograph #45 – Symbol ax

Radiograph #45 illustrates 3 examples of coalescent small opacities (images B, C, and D) and contrasts them with image A, which shows superimposition of opacities without coalescence.

Radiograph #45A. This image illustrates an excellent example of **r/r** - 3/3. The left lung shows superimposition of many small opacities but there is no coalescence. The normal vascular pattern is totally obscured. On the right, there is a category A large opacity in the right upper zone, as well as coalescence (**ax**) along the upper right lateral chest wall. Note also hilar adenopathy (**hi**).

Radiograph #45B. An area of coalescence, **ax,** is seen on this image lateral to the left hilum (arrow) overlying the left fourth anterior rib. Large opacities are evident along the right lateral chest wall as opaque densities adjacent to areas of coalescence in which the margins of small opacities are still discernible. These large opacities would be classified as category "B" since the sum of their diameters is greater than 50 mm. There is blunting of the right costophrenic angle with minimal extension superiorly, scored as diffuse pleural thickening in profile extent 1, width a. Calcified face-on plaque is visible at the right base between the 7th and 8th anterior ribs, and is separate from the costophrenic angle blunting. The left hilum is enlarged (symbol hi).

Radiograph #45C shows widespread rounded small opacities, **q/r,** with a profusion of 3/2. A good example of coalescent small opacities is seen beneath the middle left clavicular shadow (arrow), and the left base overlying the 6th anterior rib (arrow). These densities are not considered to represent a large opacity because they are not homogeneous, and the margins of the coalescing small opacities remain visible. This image also illustrates superimposition of small opacities and a large relatively homogeneous opacities opacity where the sum of the long axis diameters is greater than 50 mm, therefore category "B". Note the large opacity on the right is in the lower zone. Symbols **ax**, **bu**, **em**, **di,** and **hi** are checked.

Radiograph #45D once again shows widespread small, rounded opacities, **r/r,** and profusion of 3/+. There is an area of coalescent small opacities (**ax**) over the anterior left second rib in this image. Large opacities are classified as "B" when they are added together, and superimposition of small opacities are also present. Symbols **at, ax, and ih** are checked.

Large Opacity A

When marking the classification form, if both coalescent small opacities and an “A” large opacity are thought to be present, check both Section 2C and symbol **ax** in Section 4B. If you are uncertain whether a density represents coalescent small opacities or an “A” large opacity, check Section 2C or **ax,** whichever you think most likely, and note the possibility of the other type of abnormality in Section 4, “Other Comments.”

The classification of large opacity “A” depends on the presence of one or more relatively homogeneous opacities, each greater than 10 mm in the largest dimension and the sum of the longest dimensions not exceeding 50 mm. It may be difficult to determine the precise measurements of such opacities because, in many instances, the edges or borders may be poorly defined or obscured by adjacent structures. Such lesions may be single or multiple and are almost always associated with a background of small opacities. If hilar migration of the large opacity or adjacent bullous emphysema occurs, the small opacities tend to become less conspicuous and less profuse. An “A” opacity may be entirely ill-defined but usually presents at least one fairly well-defined border. Unilateral large opacities may have characteristics similar to those of a fluid-filled cyst or carcinoma. If carcinoma is suspected, the concern must be indicated using the obligatory symbol **ca** in Section 4B with additional comments. The appropriate physician must be notified if **ca** is selected in 4B.

Radiograph #46

Radiograph #46A shows small, rounded opacities predominately in all zones, **r/r,** and profusion of 2/2. This image shows superimposition of multiple small opacities and an area of coalescence, **ax,** in the first and second right anterior rib interspaces (arrow). Note that these areas are not homogeneous in character. No large opacity is present. Postsurgical changes in the left hemithorax are consistent with left upper lobectomy.

Radiograph #46B illustrates a well-defined large opacity, type "A," in the right upper zone. Note its flat margin laterally. There is a background of small opacities, q/r**,** predominately in the upper and middle zones with minimal involvement of the right lower zone, and no involvement of the left lower zone. Profusion was determined to be 1/2. Coalescence, **ax,** is lateral to the right hilum in the right middle zone (arrow). Note the slight distortion and emphysema adjacent to the large opacity. Since the right upper zone opacity could also represent cancer or tuberculosis, these symbols may also be checked. The "See physician" box should be checked "YES”. The symbols **di, em, and tb** are also checked.

Radiograph #46C. There is a large opacity category “B” in the right middle zone. There is the suggestion of an additional large opacity laterally in the left upper zone beneath the left clavicle. Note the elevation and distortion of the left hilum. Coalescence, **ax**, is identified at the left anterior second rib (arrow) and in the left lower zone along the lateral left diaphragm (arrow). Numerous small, rounded opacities, **r/q,** are widespread, with a profusion of **3/3**. Due to the suggestion of air space opacity in the right middle zone, an acute pneumonia or malignancy (**ca**) are considerations. The appropriate physician should be notified. The symbols **di, hi,** and **ih** are also checked.

Radiograph #46D illustrates a poorly defined opacity in the right upper zone (arrow) that meets the criteria of an "A" opacity. The background of small opacities, q/q**,** with a profusion of 1/1 is consistent with a large opacity; however, neoplasm should be considered. Once again, the appropriate physician should be notified. The symbols **ca, di,** and **pb** are checked.

Symbol ca

Cancer of the lung is the most common lethal cancer. Lung cancer survival is related to the stage at diagnosis, with a much better prognosis for those diagnosed at earlier stages. Identifying findings suspicious for lung cancer in chest radiographs and ensuring appropriate, timely notification of results can allow patients to receive timely follow-up diagnostic and therapeutic care. It is important to recognize that mineral dusts such as asbestos and crystalline silica do not only cause pneumoconiosis. The International Agency for Research on Cancer has also identified them as known human lung carcinogens. Some reports have also suggested that coal miners may be at increased risk for lung cancer mortality. The radiologic distinction between a large opacity and a malignant neoplasm is extremely difficult; the two conditions may be reported in the same chest radiograph.

It is often difficult to distinguish between large opacities and malignancy. Please consider the following:

1. A large opacity of pneumoconiosis is almost invariably associated with an unequivocal background of small pneumoconiotic opacities with a profusion level of category 1/0 or greater. As large opacities increase in size, however, they may appear to incorporate surrounding small opacities. Moreover, as they enlarge, emphysematous changes in the surrounding lung become increasingly apparent. As a result, the profusion of small opacities surrounding a large opacity may appear to diminish over time and, in rare cases, may disappear entirely.
2. The large opacity of pneumoconiosis usually has at least one sharply defined border, whereas the shadows of malignant neoplasms are often completely ill-defined. However, the margination of a shadow alone is not a reliable characteristic on which to base the distinction between a benign pneumoconiotic opacity and a malignant neoplasm.
3. Longitudinal evaluation of serial imaging may be helpful. The large opacities of pneumoconiosis may change very slowly, usually over years. Opacities representing carcinomas tend to change more rapidly.
4. If large opacities are bilateral and symmetrical, one might consider this more likely PMF rather than malignancy.

By now, you should be familiar with the form for reporting your classification of chest radiographs according to the ILO 2022 system. You have reviewed representations of the radiographic findings that are characteristic of pneumoconiosis and have learned the conventions to be observed in quantifying them. You can now apply your knowledge to the interpretation of clinical radiographs. Radiographs #47 through #83 provide you with this opportunity.

SUBSET 5 – Radiographs #47 to #83

Subset 5 consists of radiographs and answer keys. Complete one classification form for each of the radiographs in this subset. Then, compare your classifications to the validated classifications from expert readers on the answer keys provided. There may be some differences in how the radiographs are classified. However, if your classifications depart significantly from the experts', we suggest that you review the appropriate sections in Subsets 1–4.

PLEASE NOTE: Throughout this self-study syllabus you may notice minor differences between classification forms because of occasional modifications. However, the most significant components of the forms, and most importantly, the principles of classification, remain the same.

Reminder: The PDF portfolio of answer keys is a separate PDF portfolio.

Radiographs 74, 78, and 80 were removed and are not contained in this syllabus.

We hope you have found this self-study syllabus useful as you prepare for the B Reader examination. When you are satisfied that you have mastered the information and are interested in taking the B Reader certification or recertification examination, please visit the NIOSH website (NIOSH B Reader Program | Radiographic ScreeningNIOSH B Reader Program | Radiographic Screening | CDC | CDC) for additional information or contact the B Reader program at the address below:

Respiratory Health Division
Coal Workers' Health Surveillance Program
Workforce Screening and Surveillance Team
Surveillance Branch
cwhsp@cdc.gov
(304) 285-5724

Study Syllabus Quiz

1. Which of the following judgments is required BEFORE a reader completes Sections 2A and 3A of the NIOSH form?

A) Any pleural or parenchymal findings are consistent with pneumoconiosis

B) The radiographic findings are not consistent with pneumoconiosis

C) Radiographic changes are most likely due to pneumoconiosis

D) It is necessary to establish whether or not a worker is entitled to compensation

Answer A

For most purposes, the appearances should be classified if the reader considers that the findings might be due to dust exposure, or that they are consistent with pneumoconiosis. It is not necessary for the reader to judge whether the changes are most likely due to pneumoconiosis. Readers may be instructed to classify only those appearances that they believe or suspect to be pneumoconiotic in origin.

2. Regarding the technical quality of a radiograph to be classified using the ILO system (Section 1, Film Quality):

A) Assessing the technical quality of a radiograph is optional, but recommended

B) Assessing the technical quality of a radiograph is required, but it is not necessary to specify the defect on the interpretation form

C) if a technical defect is noted, it should be specified on the reading form

D) Images of quality grade 2 have defects that are likely to affect the classification process

Answer C

Specifying the nature and severity of an image's technical defects allows an assessment of their potential impact on the classification, and also permits the x-ray facility to specifically address improvement of image quality. Image quality grade 2 indicates an acceptable image with no technical defects or artifacts likely to impair classification of the radiograph for pneumoconiosis.

3. Regarding the naming conventions of the ILO system for small opacities due to dust:

A) Rounded small opacities are labeled s, t, or u

B) Irregular small irregular opacities are labeled p, q, or r

C) The widths of “t” opacities and diameters of “q” opacities range from 1.5 to 3 mm

D) The size of irregular small opacities is determined by their length

Answer C
The widths of opacities labeled t and the diameters of opacities labeled q range from over 1.5 mm to about 3 mm in diameter.

Irregular small opacities are labeled s, t, or u. Rounded small opacities are labeled p, q, or r. The size of irregular small opacities is determined by their width.

4. How are lung zones defined for reporting the profusion of small opacities?

A) Each lung is divided into six zones

B) Each lung is divided into upper, middle, and lower zones

C) Lung zones are labeled A, B, and C from top to bottom

D) Lung zones are labeled 1, 2, and 3 from top to bottom

Answer B
Each lung is divided into three zones: upper, middle, and lower.

5. When categorizing small-opacity profusions, which of the following is the correct way to determine the overall ILO profusion category?

A) As the profusion category increases from 0 to 3, the number of opacities per unit area decreases

B) The lung vessels are seen progressively more clearly as the profusion category increases

C) If a reader indicates that the profusion category is 1/0, the reader seriously considered the category 0/0 ILO Standard but judged the radiograph to more closely resemble the category 1/1 ILO Standard

D) The overall profusion category that is marked on the reading sheet should be mentally calculated as the average of all zones, including zones that are not affected by pneumoconiosis

Answer C

In determining the overall profusion category, the reader should average only the zones that are affected and whose profusion is within 2 or fewer subcategories of the most affected zone.

As the profusion category increases from 0 to 3, the number of opacities per unit area increases. The lung vessels are seen progressively less clearly as the profusion category increases. In determining the overall profusion category, the reader should average only the zones that are affected and whose profusion is within 2 or fewer subcategories of the most affected zone.

6. Regarding the classification of large pneumoconiotic opacities:

A) Classification A denotes an opacity whose greatest diameter exceeds 20 mm but is less than 60 mm

B) Coalescence of small opacities is classified the same as type A large opacity, provided the small opacities are homogeneous in appearance

C) A large opacity can be labeled C only if it occurs in the right upper zone

D) Large opacities usually occur in the presence of a background of small opacities

Answer D

Classification A denotes an opacity whose greatest diameter exceeds 10 mm but is less than 50 mm. The symbol “ax” refers to an area of coalescence of small pneumoconiotic opacities (rounded or irregular) within which the margins of the individual opacities are still identifiable; a true large opacity has a more homogeneous appearance. Classification C denotes a large opacity whose area exceeds that of the right upper zone, or several large opacities whose areas when summed exceed the area of the right upper zone.

7. In which of the following locations are localized plaques reported to LEAST occur from asbestos exposure?

A) Both hemidiaphragms

B) The lateral chest wall

C) Along the mediastinum

D) In the trachea and main bronchi

Answer D

Localized plaques associated with asbestos exposure are most frequently reported in both hemidiaphragms, the lateral chest wall and along the mediastinum.

8. Concerning the classification of pleural plaques and diffuse pleural thickening:

A) A pleural thickening of width category A ranges from 0 to 5 mm in width

B) A face-on plaque is seen sharply along either the right or left lateral chest wall

C) The width refers to the vertical length, or the sum of the lengths of the plaques present

D) In any location where pleural calcification is noted, a plaque should also be recorded

Answer D

Width category A ranges from at least 3 mm up to 5 mm. In-profile plaque is seen sharply along either the right or left lateral chest wall. Extent refers to the vertical length, which is the sum of the lengths of the plaques present. The width of in-profile plaque is measured as the maximum distance from the inner rib border of the lateral chest wall to the sharp inner margin of the plaque.

9. Concerning the correct classification of costophrenic angle obliteration:

A) It should be recorded when the angle is less obliterated than in the CPa standard radiograph.

B) Diffuse pleural thickening should be recorded as present in a hemithorax in the absence of associated obliteration of the costophrenic angle

C) Costophrenic angle obliteration can be recorded either with or without associated diffuse pleural thickening of the chest wall

D) Even marked costophrenic angle obliteration should be recorded provided it is clearly related to chest wall trauma

Answer C

Costophrenic angle obliteration should NOT be recorded when the angle is less obliterated than the CPa standard radiograph. By convention, diffuse pleural thickening cannot be present in a hemithorax in the absence of obliteration of the costophrenic angle. Even marked costophrenic angle obliteration is not to be recorded unless it is thought to be potentially related to pneumoconiosis (ie, not chest wall trauma).

10. Which of the following is the correct use of obligatory symbols in classifying other abnormalities?

A) Mesothelioma should be coded “mo”

B) Calcified primary tuberculosis with a hilar calcification is properly coded “tb”

C) A thickened minor fissure is coded “pi”

D) Significant atelectasis is coded “at”

Answer C

Mesothelioma should be coded “me”. The symbol “tb” should be used for tuberculosis excluding the calcified primary complex, which is coded as calcified granuloma “cg.” The symbol “at” is for significant apical pleural thickening, “pa” represents plate-like atelectasis, and “ra” is used for rounded atelectasis.

11. Which of the following judgments are required before a reader marks any of the 28 obligatory symbols in Section 4B of the ILO form?

A) The radiographic findings are suggestive of the condition

B) The radiographic findings are most likely due to the condition

C) The radiographic findings are diagnostic of the condition

D) The radiographic findings should be confirmed on CT

Answer A

The correct answer is A. The ILO acknowledges that in many cases, radiographic features are not sufficient to justify a definitive interpretation of the abnormalities indicated by the symbols, and suggests that the descriptions of each of the symbols should be preceded by the words “suspect” or “opacities suggestive of”

12. What is the overall purpose of Section 4 of the classification form?

A) To record the name and address of the subject

B) To record the obligatory other symbols and to indicate the presence and additional descriptions of significant abnormalities or other diseases noted on the radiograph

C) To document ILO standard radiographs that were reviewed in completing the form

D) To provide a description of the suspected cause of the pneumoconiotic opacities

Answer B

To record the obligatory other symbols and to indicate the presence and additional descriptions of significant abnormalities or other diseases noted on the radiograph.

13. If a reader notes significant non-pneumoconiotic abnormalities other than the obligatory symbols, what procedure should be followed when completing the classification form?

A) Do not mark a box; do not describe findings in the comments section of the form

B) Mark OD (other disease or significant abnormality) and add written comments about the abnormalities in the margins of the form.

C) Mark PX and describe findings in the comments section of the form

D) Mark OD and describe findings in the comments section of the form

Answer D
Mark OD and describe findings in the comments section of the form.